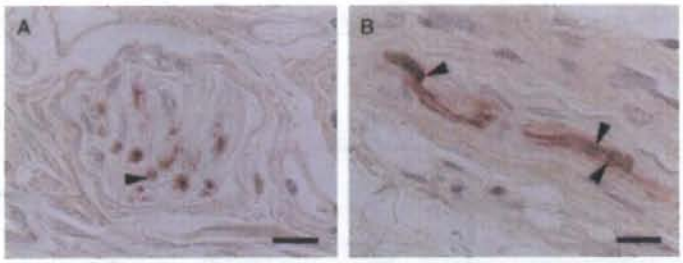

FIGURE 2. Double immunocytochemical staining with anti-phosphorylated α-synuclein (brown) and anti-phosphorylated neurofilament (red) antibodies. **(A)** In a cross section, PSer129 immunoreactivity is localized within SMI31-immunoreactive axons (arrowhead). **(B)** In a longitudinal section of a nerve fascicle, PSer 129 immunoreactivity is continuous with SMI31-immunoreactive axons (arrowheads). Scale bars = **(A, B)** 10 μm.

axons. This was confirmed by double label immunohistochemistry using antibodies to psyn and phosphorylated neurofilament (Figs. 2A, B). By confocal microscopy, psyn immunoreactivity was also colocalized with the epitope of anti-TH antibody (Fig. 3).

By electron microscopy of immunostained sections, psyn-immunoreactive structures seemed to be composed of granulofilamentous profiles among mitochondria and vesicles. The psyn-immunoreactive structures had thin filaments at their peripheries that were consistent with the size of intermediate filaments and were surrounded by basal lamina. These features are consistent with those of unmyelinated axons (Fig. 4).

Comparison of CNS LB Stages

Psyn-positive structures in the skin were very small and not always found in the 2 serial sections stained either with psyn no. 64 and PSer129. Therefore, when positive immunoreactivity was found in any of the 2 stained sections for each anatomical location, the case was counted as positive. Correlations between CNS LB stage in the prospective study and the presence or absence of α-synuclein immunoreactivity in the skin are summarized in Table 3. Psyn immunoreactivity in abdominal and brachial skin did not always match in a single patient (Table 3), but the overall frequencies were similar and were apparently unaffected by differences in the method of fixation or in anatomical location.

The numbers of patients and rates of skin positivity (%) at each stage were as follows: stage 0, none of 194 patients (0%); stage 0.5, 1 (4.0%) of 25 patients; stage I, 1 (3.7%) of 27 patients; stage II, 3 (33.3%) of 9 patients; stage III, 2 (100%) of 2 patients; stage IV, 6 (54.5%) of 11 patients; and stage V, 7 (63.6%) of 11 patients. Because all CNS LB stage 0 patients, including 8 progressive supranuclear palsy and 3 corticobasal degeneration cases, were negative for psyn immunoreactivity in the skin, there were no false-positive results, and the specificity was 100%. Among the 20 patients with psyn-positive immunoreactivity in the skin, 11 had positive immunoreactivity in both skin locations, 6 in the abdominal skin alone, and 3 in the skin of the arm alone.

Comparison With Adrenal Gland Positivity

All the patients with positive psyn immunoreactivity in the skin also had α-synucleinopathy in the adrenal glands (Table 3).

Retrospective Study

Pathology of LB-Related α-Synucleinopathy in the Skin

The numbers of patients and the rates of skin positivity (percentage) at each CNS LB stage of II or more were as follows: stage II, 13 (23.2%) of 56 patients; stage III, 10 (71.4%) of 14 patients; stage IV, 17 (44.7%) of 38 patients; stage V, 18 (52.9%) of 34 patients (Table 4). Samples from all 3 of the patients with MSA were negative.

We next examined the percentages of patients with positive psyn immunoreactivity in the skin from the abdomen in each subgroup of CNS LB stage II or subclinical LBD (Table 4). The sensitivity was approximately 20%, but was 0% for the amygdala variant cases. We then classified stage IV and V cases into PDD and DLB and compared the

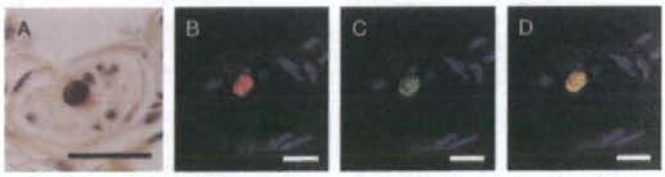

FIGURE 3. Immunohistochemical and confocal immunofluorescent localization of phosphorylated α-synuclein (PSer129) and tyrosine hydroxylase (TH). **(A)** An oval area of immunoreactivity to PSer129 in the dermal nerve. Scale bars = 25 μm. **(B–D)** Confocal images of dermal nerve showing colocalization. **(B)** Alexa 546 (red) for phosphorylated α-synuclein. **(C)** Alexa 488 (green) for TH. **(D)** View of merged **(B** and **C)**. Scale bars = **(B–D)** 10 μm.

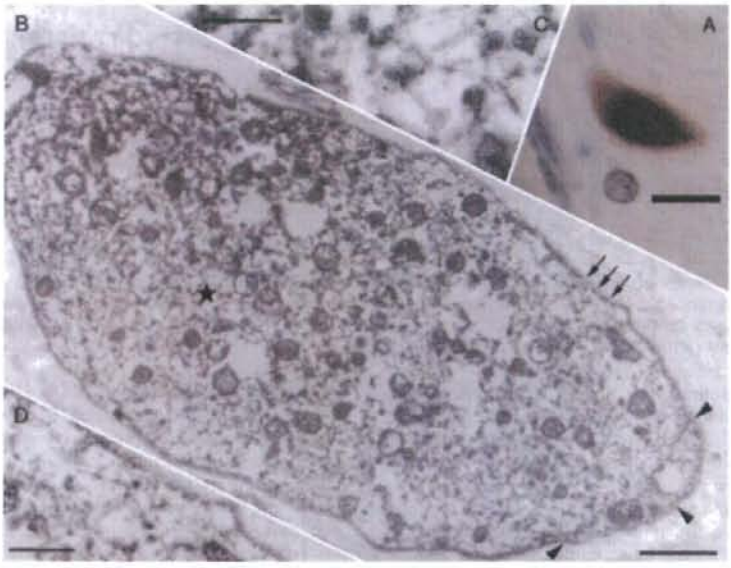

FIGURE 4. Immunoelectron microscopy of anti-phosphorylated α-synuclein antibody (PSer129)–immunoreactive structures in a dermal nerve fascicle. **(A)** Light microscopy of an immunoreactive oval profile visualized with diaminobenzidine. Scale bars = 25 μm. **(B)** Immunoelectron microscopy showing the structure shown in **(A)** surrounded by basal lamina (triple arrows) and with abundant organelles. This probably represents the cytoplasm of an unmyelinated Schwann cell (arrowheads). Scale bars = 1 μm. **(C)** High-magnification view of the area indicated by the asterisk in **(B)**, demonstrating granulofilamentous profiles among mitochondria and vesicular structures. Scale bars = 250 nm. **(D)** High-magnification view of the area indicated by the arrows in **(B)** showing thin filaments. Scale bars = 500 nm.

positivity ratios. The number of patients and positivity ratio (%) in each group were as follows: PDDT, 8 (61.5%) of 13 patients; DLBT, 9 (36%) of 25 patients; PDDN, 6 (85.7%) of 7 patients; and DLBN, 12 (44.4%) of 27 patients. Therefore, the sensitivity of LB pathology in the skin was 14 (70%) of 20 in PDD and 21 (40.4%) of 52 in DLB.

Association of Coexistent Pathology of AD or Argyrophilic Grain Disease With LB-Related Skin Pathology in PDD or DLB

Patients with PDD or DLB were classified into 2 groups: those having or not having LB-related pathology in the skin. These 2 groups were evaluated for the grade of coexistent AD

TABLE 3. Lewy Body Pathology in the Skin of the 279 Consecutive Patients Used in the Prospective Study

		LB Pathology in the Skin				Adrenal LBD
CNS LB Stage	n	Arm +/Abdomen +	Arm +/Abdomen −	Arm −/Abdomen +	Positive, %	Positive, %
0	194	0	0	0	0	1 (0.5)
0.5	25	0	0	1	1 (4.0)	1 (4.0)
I	27	0	0	1	1 (3.7)	2 (7.4)
II	9	1	1	1	3 (33.3)	6 (66.7)
III	2	2	0	0	2 (100)	2 (100)
IV	11	4	1	1	6 (54.5)	11 (100)
P	4	1	0	0	1	4 (100)
D	7	3	1	1	5	7 (100)
V	11	4	1	2	7 (63.6)	10 (90.9)
P	1	0	1	0	1	1 (100)
D	10	4	0	2	6	9 (90)
Total	279	11	3	6	20	33

Because no LB pathology was detected in the skin in cases without CNS LB pathology, the specificity of dermal LB pathology with respect to the CNS was 100%.
Abdomen, abdominal wall; Arm, flexor surface of the upper arm; D, dementia with LBs; LB, Lewy body; LBD, Lewy body disease; P, Parkinson disease with dementia.

or argyrophilic grain disease (AGD) pathology. Nine (25.7%) of 35 PDD/DLB cases with psyn immunoreactivity in the skin were complicated by AD pathology or Braak neurofibrillary tangle stage equal to or more than III and senile plaque stage equal to C (21). In contrast, 14 of 37 anti-psyn negative PDD/DLB cases (37.8%) were complicated by AD pathology (Table 5). Seven (20%) of 35 PDD/DLB cases with LB pathology of the skin were complicated by AGD stage II or greater. Twelve (32.4%) of 37 cases without LB pathology in the skin were complicated by AGD stage II or greater. Thus, AD pathology or high-grade AGD pathology complicated 14 (40%) of 35 psyn-positive cases and 25 (67.6%) of 37 psyn-negative cases. The rate of complication by AD and/or AGD pathology was significantly higher in PDD/DLB patients without dermal α-synucleinopathy than in PDD/DLB patients with accompanying LB-related pathology in the skin ($p = 0.019$; Table 5).

Clinicopathologic Correlation of Subclinical and Clinical LBD With LB Pathology in the Skin

Activities of daily living (ADL) data on the 84 patients without dermal LB-related pathology in the retrospective study were as follows: bedridden, 39 patients (46.4%); wheelchair-bound, 6 patients (7.1%); cane-assisted, 13 patients (15.5%); and walking independently, 26 patients (31.0%). The ADL data on the 58 patients with dermal LB-related pathology were as follows: bedridden, 37 patients (63.8%); wheelchair-bound, 7 patients (12.1%); cane-assisted, 4 patients (6.9%); and walking independently, 10 patients (17.2%). The proportion of bedridden patients was significantly higher ($p < 0.001$) and the proportion of patients walking independently tended to be lower ($p = 0.065$) among psyn-positive patients compared with psyn-negative patients. The numbers of bedridden patients with decubitus ulcers were as follows: dermal psyn-negative patients, 14 (35.6%) of 39; dermal psyn-positive patients, 21 (56.8%) of 37. Thus, patients with positive dermal LB pathology had a significantly higher rate of decubitus ulcers than dermal LB-negative patients ($p = 0.028$).

TABLE 4. Lewy Body Pathology in the Abdominal Skin in Subclinical and Clinical LBD

LB Stage	Subtype	n	Dermal LBD, %	Adrenal LB, %
II		56	13 (23.2)	42 (75)
	B	16	3 (18.8)	12 (75)
	T	34	9 (26.5)	26 (76.5)
	N	4	1 (25.0)	4 (100)
II	A	2	0	0
III		14	10 (71.4)	14 (100)
	B	9	6 (66.7)	9 (100)
	T	3	2 (66.7)	3 (100)
	N	2	2 (100)	2 (100)
IV		38	17 (44.7)	33 (100)
P	PDDT	13	8 (61.5)	13 (100)
D	DLBT	25	9 (36.0)	20 (80)
V		34	18 (52.9)	30 (88.2)
P	PDDN	7	6 (85.7)	7 (100)
D	DLBN	27	12 (44.4)	23 (85.2)

Differential diagnosis of PDD and DLB was based on the "1-year rule" in the consensus guidelines (19). Subtype was based on LB score: B, brainstem; T, transitional; and N, neocortical. A, Amygdala variant, represents LB pathology centered around amygdala and lacking involvement of the peripheral autonomic nervous system (2).

D, dementia with LBs; DLBN, dementia with LBs, with an LB score corresponding to the value for the neocortical form; DLBT, dementia with LBs, with an LB score corresponding to the value for the transitional form; LB, Lewy body; LBD, LB disease; P, PD with dementia; PD, Parkinson disease; PDDN, PD with dementia, with an LB score corresponding to the value for the neocortical form; PDDT, PD with dementia, with an LB score corresponding to the value for the transitional form.

TABLE 5. Influence of Coexistent Pathology in the Form of AD or AGD on LB Pathology Involving the Skin in Patients with PDD or DLB

		n	AD(+)	AGD(+)	Total*
Skin psyn(+)	Total	35	9 (25.7%)	7 (20%)	14 (40%)
	PDD	14	2	2	4
	DLB	21	7	5	10
Skin psyn(−)	Total	37	14 (37.8%)	12 (32.4%)	25 (67.6%)
	PDD	6	0	3	2
	DLB	31	14	10	23

*Number of cases complicated by either AD or AGD.

AD, Alzheimer disease; AGD, argyrophilic grain disease; DLB, dementia with LBs; PDD, Parkinson disease with dementia.

DISCUSSION

This study is the first to demonstrate that LB-related pathology involves the cutaneous nerves in LBD. Because LB-related pathology identified in the skin was only seen in cases that had LB-related pathology in the CNS and not in 194 cases without CNS LB-related pathology, there were no false-positives; the specificity is, therefore, 100%. The sensitivity of LB pathology in the skin was 70% in PD and 40% in DLB in single sampling from the abdominal surface. The PDD or DLB cases without LB-related pathology in the skin were more frequently complicated by AD or AGD pathology than were those with LB-related pathology in the skin.

Sympathetic nerve fibers innervate blood vessels, eccrine glands, and the erector pili muscles in the skin. Sympathetic nerve fibers that innervate eccrine glands are cholinergic nerves, whereas all others are adrenergic. The psyn-positive structures were colocalized with axons visualized with SMI31 in the skin and were associated with axons by electron microscopy and TH immunohistochemistry. In light of these findings, we speculate that the psyn immunoreactivity was localized in the adrenergic nerves that innervate blood vessels and erector pili muscles in the skin. Not all psyn immunoreactivities were colocalized with anti-TH-immunoreactive axons, however, and it is more probable that α-synuclein also accumulates in the cholinergic nerves that innervate eccrine glands.

By electron microscopy, classic perikaryonal and intraneuritic LBs in the CNS are composed of a dense central core and surrounded by radiating filaments and vesicles. The LBs in the axons consist of randomly arranged or aggregated filamentous material with an inner core composed of electron-dense granular material. Immunohistochemical studies with anti-psyn antibodies have demonstrated axonal swellings in the cerebral white matter (16); these axonal swellings

contained mitochondria and dense and lamellated bodies ultrastructurally (data not shown). Our electron microscopic findings of psyn-immunoreactive structures in the skin seem to be similar to those of axonal swellings in the CNS. This suggests that the cutaneous nerves were directly affected by LB-type accumulation of psyn.

Tests such as the thermal sweat test, pilocarpine sweat test, and sympathetic skin response have been used clinically to evaluate sudomotor function. There have been some clinical reports of the use of these tests to gauge sudomotor function in PD, but the severity and distribution of sudomotor dysfunction differ between each study (24–26). Studies suggest that the central or preganglionic sympathetic fibers may be involved in the early-stage lesions responsible for sudomotor dysfunction; postganglionic sympathetic fibers may become involved with progression of the disease. There have been few pathological studies of the skin in LBD (27), and no reports have described LB-related pathology in the skin. Our studies provide definite morphological evidence of the involvement of postganglionic axon terminals in LBD.

There is controversy regarding the distribution of clinical sudomotor dysfunction in LBD. Most reports indicate that although sweating preferentially decreases in the distal extremities, the distribution of the sudomotor dysfunction is patchy and differs among patients. Our prospective studies of the brachial and abdominal skin showed that psyn immunoreactivity was not always the same in skin from 2 different anatomical locations. Because the distal extremities were frequently affected by ischemic changes in our elderly cohort, we chose a proximal extremity and the trunk for the evaluation of LBD pathology. If skin biopsy is to become a useful tool in the diagnosis of LBD, it will be necessary to choose an area of skin where physiological tests consistently show definite abnormalities. Low sensitivity (about 20%) of dermal LB pathology among subclinical LBD cases (our CNS LB stage II) may also indicate that random skin biopsy is not valid for the early diagnosis of LBDs.

We retrospectively investigated possible correlations between the patients' ADL and skin LB pathology and found that ADL criteria were worse in patients with positive LB-related pathology in the skin than in those without it. This result is consistent with the clinical consensus in LBD that autonomic dysfunction usually parallels motor signs. Moreover, dermal psyn-positive patients had a significantly higher rate of complications in the form of decubitus ulcers than did the negative patients. Although the main cause of decubitus ulceration relates to motor disturbance in LBD patients, the direct involvement of the skin by LBD may be a contributing factor that warrants additional attention.

Our results also reveal that the epitope of phosphorylated α-synuclein accumulates in the cutaneous nerves in subclinical LBD. This finding is consistent with cardiac 123I-metaiodobenzylguanidine scintigraphic finding of involvement of unmyelinated fibers in the epicardial fatty tissue in incidental LBD (28).

Dermal psyn immunoreactivity was observed most frequently in PD (without dementia) and reached 100% in the prospective study, although the number of cases was small. In CNS LB stages IV and V, LB-related pathology in the skin was more frequent in PDD than in DLB. In addition, PDD and DLB cases without cutaneous LB-related pathology were more frequently complicated by the pathology of AD or AGD. Braak et al (29) proposed a staging paradigm whereby LB-related pathology first occurs in the dorsal motor nucleus of the vagus nerve, extends rostrally in the brainstem, reaches the limbic system, and eventually affects the cerebral cortex. Cumulative evidence indicates that LB-related pathology preferentially localizes itself in the amygdala in AD (30) and other tauopathies (14); this pattern of distribution has been termed the *amygdala variant* (2). We previously found that the adrenal glands were always free of LB-related pathology in such cases of amygdala variant (2). Although in the present study the number of cases was small, the skin was always free of LB-related pathology in the cases of *amygdala variant* studied (Table 4). These data further support our hypothesis that the presence of other dementing pathology in the CNS, such as AD or AGD, may induce cerebrally predominant distribution of LB pathology with relative sparing of the PANS.

One of the 279 patients in the prospective study presented with many LB-related pathological features in the abdominal skin and LBs in the adrenal glands but only very few Lewy neurites and dots in the dorsal motor nucleus of the vagus in the CNS. This case might represent the earliest stage of LBPAF.

For the differential diagnosis among parkinsonian syndromes, we additionally examined 3 more cases with MSA (2 MSA-P and 1 MSA-C patients) since 2006 and confirmed negative results. Although more cases should be analyzed for further confirmation and assessment of specificity, anti-psyn immunoreactivity of the skin was only positive for LBD and negative for MSA, progressive supranuclear palsy, and corticobasal degeneration in this study.

In conclusion, we document LB-related pathology involvement in cutaneous nerves in LBD. Skin biopsy may, therefore, have diagnostic application in cases of PD or LBPAF with advanced autonomic failure.

ACKNOWLEDGMENTS

The authors thank Mr Naoo Aikyo, Ms Mieko Harada, Mr Satoru Fukuda, and Ms Nobuko Naoi (Department of Neuropathology, Tokyo Metropolitan Institute for Gerontology) for the preparation of sections and Dr Kinuko Suzuki for helpful discussions. We also thank 2 anonymous neurologists for preparing the Clinical Dementia Rating scale used in this study.

REFERENCES

1. Kosaka K, Yoshimura M, Ikeda K, et al. Diffuse type of Lewy body disease: Progressive dementia with abundant cortical Lewy bodies and senile changes of varying degree—a new disease? Clin Neuropathol 1984;3:185–92
2. Fumimura Y, Ikemura M, Saito Y, et al. Analysis of the adrenal gland is useful for evaluating pathology of the peripheral autonomic nervous system in Lewy body disease. J Neuropathol Exp Neurol 2007;66: 354–62
3. Wakabayashi K, Takahashi H, Takeda S, et al. Parkinson's disease: The presence of Lewy bodies in Auerbach's and Meissner's plexuses. Acta Neuropathol (Berl) 1988;76:217–21
4. Wakabayashi K, Takahashi H, Ohama E, et al. Parkinson's disease: An

immunohistochemical study of Lewy body–containing neurons in the enteric nervous system. Acta Neuropathol (Berl) 1990;79:581–83
5. Qualman SJ, Haupt HM, Yang P, et al. Esophageal Lewy bodies associated with ganglion cell loss in achalasia. Gastroenterology 1984; 87:848–56
6. Wakabayashi K, Takahashi H. Neuropathology of autonomic nervous system in Parkinson's disease. Eur Neurol 1997;38(Suppl 2):2–7
7. Wakabayashi K. Parkinson's disease: The distribution of Lewy bodies in the peripheral autonomic nervous system. No To Shinkei 1989;41:965–71
8. Den Hartog Jager WA, Bethlem J. The distribution of Lewy bodies in the central and autonomic nervous systems in idiopathic paralysis agitans. J Neurol Neurosurg Psych 1960;23:283–90
9. Orimo S, Oka T, Miura H, et al. Sympathetic cardiac denervation in Parkinson's disease and pure autonomic failure but not in multiple system atrophy. J Neurol Neurosurg Psych 2002;73:776–77
10. Orimo S, Ozawa E, Nakade S, et al. (123)I-metaiodobenzylguanidine myocardial scintigraphy in Parkinson's disease. J Neurol Neurosurg Psych 1999;67:189–94
11. Mitsui J, Saito Y, Momose T, et al. Pathology of the sympathetic nervous system corresponding to the decreased cardiac uptake in 123I-metaiodobenzylguanidine (MIBG) scintigraphy in a patient with Parkinson disease. J Neurol Sci 2006;243:101–4
12. Forno LS, Norville RL. Ultrastructure of Lewy bodies in the stellate ganglion. Acta Neuropathol (Berl) 1976;34:183–97
13. Saito Y, Ruberu NN, Sawabe M, et al. Staging of argyrophilic grains: An age-associated tauopathy. J Neuropathol Exp Neurol 2004;63: 911–18
14. Saito Y, Ruberu NN, Sawabe M, et al. Lewy body-related a-synucleinopathy in aging. J Neuropathol Exp Neurol 2004;63:742–49
15. Saito Y, Nakahara K, Yamanouchi H, et al. Severe involvement of ambient gyrus in dementia with grains. J Neuropathol Exp Neurol 2002; 61:789–96
16. Saito Y, Kawashima A, Ruberu NN, et al. Accumulation of phosphorylated alpha-synuclein in aging human brain. J Neuropathol Exp Neurol 2003;62:644–54
17. Fujiwara H, Hasegawa M, Dohmae N, et al. a-Synuclein is phosphorylated in synucleinopathy lesions. Nat Cell Biol 2002;4:160–64
18. McKeith IG, Dickson DW, Lowe J, et al. Diagnosis and management of dementia with Lewy bodies: Third report of the DLB Consortium. Neurology 2005;65:1863–72
19. McKeith IG, Galasko D, Kosaka K, et al. Consensus guidelines for the clinical and pathologic diagnosis of dementia with Lewy bodies (DLB): Report of the Consortium on DLB international workshop. Neurology 1996;47:1113–24
20. Braak H, Braak E. Neuropathological staging of Alzheimer-related changes. Acta Neuropathol (Berl) 1991;82:239–59
21. Murayama S, Saito Y. Neuropathological diagnostic criteria for Alzheimer's disease. Neuropathology 2004;24:254–60
22. Jellinger KA. Dementia with grains (argyrophilic grain disease). Brain Pathol 1998;8:377–86
23. Jellinger KA, Bancher C. Senile dementia with tangles (tangle predominant form of senile dementia). Brain Pathol 1998;8:367–76
24. Kihara M, Kihara Y, Tukamoto T, et al. Assessment of sudomotor dysfunction in early Parkinson's disease. Eur Neurol 1993;33:363–65
25. Mano Y, Nakamuro T, Takayanagi T, et al. Sweat function in Parkinson's disease. J Neurol 1994;241:573–76
26. Turkka JT, Myllyla VV. Sweating dysfunction in Parkinson's disease. Eur Neurol 1987;26:1–7
27. Dabby R, Djaldetti R, Shahmurov M, et al. Skin biopsy for assessment of autonomic denervation in Parkinson's disease. J Neural Transm 2006; 113:1169–76
28. Orimo S, Takahashi A, Uchihara T, et al. Degeneration of cardiac sympathetic nerve begins in the early disease process of Parkinson's disease. Brain Pathol 2007;17:24–30
29. Braak H, Del Tredici K, Rub U, et al. Staging of brain pathology related to sporadic Parkinson's disease. Neurobiol Aging 2003;24:197–211
30. Lippa CF, Fujiwara H, Mann DM, et al. Lewy bodies contain altered a-synuclein in brains of many familial Alzheimer's disease patients with mutations in presenilin and amyloid precursor protein genes. Am J Pathol 1998;153:1365–70

J Neuropathol Exp Neurol

Vol. 67, No. 11
November 2008
pp. 1072–1083

ORIGINAL ARTICLE

Incidence and Extent of Lewy Body–Related α-Synucleinopathy in Aging Human Olfactory Bulb

Renpei Sengoku, MD, Yuko Saito, MD, PhD, Masako Ikemura, MD, PhD, Hiroyuki Hatsuta, MD, Yoshio Sakiyama, MD, PhD, Kazutomi Kanemaru, MD, PhD, Tomio Arai, MD, PhD, Motoji Sawabe, MD, PhD, Noriko Tanaka, PhD, Hideki Mochizuki, MD, PhD, Kiyoharu Inoue, MD, PhD, and Shigeo Murayama, MD, PhD

Abstract

We investigated the incidence and extent of Lewy body (LB)–related α-synucleinopathy (LBAS) in the olfactory bulb (OB) in 320 consecutive autopsy patients from a general geriatric hospital (mean age, 81.5 ± 8.5 years). Paraffin sections were immunostained with anti-phosphorylated α-synuclein, tyrosine hydroxylase, phosphorylated tau, and amyloid β antibodies. LBAS was found in 102 patients (31.9%) in the central nervous system, including the spinal cord; the OB was involved in 85 (26.6%). Among these 85 patients, 2 had LBAS only in the anterior olfactory nucleus, 14 in the peripheral OB only, and 69 in both areas. In 5 patients, Lewy bodies were found only in the OB by hematoxylin and eosin stain; 3 of these patients had Alzheimer disease, and all had LBAS. Very few tyrosine hydroxylase–immunoreactive periglomerular cells exhibited LBAS. All 35 LBAS patients with pigmentation loss in the substantia nigra had LBAS in the OB. LBAS in the amygdala was more strongly correlated with LBAS in the anterior olfactory nucleus than with that in the OB periphery. LBAS did not correlate with systemic tauopathy or amyloid β amyloidosis. These results indicate a high incidence of LBAS in the aging human OB; they also suggest that LBAS extends from the periphery to the anterior olfactory nucleus and results in clinical manifestations of LB disease.

Key Words: α-Synuclein, Anterior olfactory nucleus, Dementia with Lewy bodies, Incidental Lewy bodies, Olfactory bulb, Parkinson disease.

From the Department of Neuropathology (RS, YS, MI, HH, YS, SM), Tokyo Metropolitan Institute of Gerontology; Department of Neurology (RS, KI), The Jikei University School of Medicine; Departments of Pathology (YS, TA, MS) and Neurology (KK), Tokyo Metropolitan Geriatric Hospital, Tokyo, Japan; Department of Biostatistics (NT), Harvard School of Public Health, Boston, Massachusetts; and Department of Neurology (HM), Juntendo University, Tokyo, Japan.

Send correspondence and reprint requests to: Shigeo Murayama, MD, PhD, Department of Neuropathology, Tokyo Metropolitan Institute of Gerontology, 35-2 Sakaecho, Itabashi-ku, Tokyo 173-0015, Japan; E-mail: smurayam@tmig.or.jp

This study was supported by the Aid for Scientific Research Basic B (S.M. and Y.S.), Basic C (Y.S.), and Priority Areas (Advanced Brain Science Project) (S.M. and Y.S.) from the Ministry of Education, Culture, Sports, Science, and Technology of Japan.

INTRODUCTION

Olfaction is a major target of neuroscience research, and numerous genes are expressed for olfactory receptors (1,000 in mouse and 300 in human) (1–3). Patients with schizophrenia exhibit olfactory dysfunction (4–7) and loss of volume of the olfactory bulb (OB) (8). Olfactory dysfunction is also an early sign of Alzheimer disease (AD) and Lewy body (LB) diseases (i.e. Parkinson disease [PD], PD with dementia [PDD], and dementia with LB [DLB]) (9–19) and has been used to differentiate these disorders from progressive supranuclear palsy (20). Atrophy of the OB as revealed by magnetic resonance imaging has been reported to be useful diagnostic tools for AD (21) and PD (22). Recently, neuroprogenitor cells that migrate from the subventricular zone were identified in the human OB (23). Twice as many tyrosine hydroxylase (TH)–immunoreactive neurons were reported in the OBs of PD patients compared with those of age- and sex-matched controls (24). Thus, it is of interest as to whether LB-related α-synucleinopathy (LBAS) involves the TH system in the OB.

Subsequent to the staging system for diffuse LB disease proposed by Kosaka (25), Braak et al (26) suggested a neuropathologic staging procedure for idiopathic PD in an aged cohort that included PDD patients but not DLB or other patients with dementia and LB pathology. The latter subgroup included the amygdala variant of LB disease (27) complicated by AD (28, 29) or other tauopathies (29). According to Braak et al, the LBAS in the central nervous system (CNS) first affects the medulla oblongata, rostrally extends to the locus coeruleus, and reaches the substantia nigra. Braak et al (30) also reported a pattern of extension from the OB to the amygdala, but neither Kosaka et al nor Braak et al (30) examined possible statistical correlations between these 2 patterns in the extension of LBAS.

In light of these previous studies, we began to include the OB in routine neuropathologic examinations and noticed that LBAS in the OB is dominant either in the anterior olfactory nucleus (AON) or in the peripheral OB. Among several anatomical nomenclature systems of OB (31–34), we adopted that of Price (34) as follows: The axons of the bipolar receptor cells (approximately 6 million per nose) in the olfactory epithelium (the primary olfactory structure) ramify in the most superficial layer of the OB, the olfactory nerve layer. They

then form synapses with the dendrites of the secondary olfactory structure that consists of mitral and tufted cells in the glomerular layer. The external plexiform layer contains the dendrites of the mitral cells and the somata of the tufted cells. The mitral cell layer is formed by the somata of the mitral cells. The axons of the mitral cells run through the internal plexiform layer and reach the granule cell layer (Fig. 1). These secondary olfactory structures are the major anatomical regions that exhibit LBAS in the OB periphery. The AON is located in the OB and olfactory peduncle; it includes several groups of pyramidal-like cells and is termed tertiary olfactory structures.

The goal of this study was to clarify the significance of LBAS involving the OB in human aging. The OB periphery (including axon terminals of the primary structure and the soma, dendrites, and axons of the secondary structure) and AON (the axon terminals of the secondary structure and the soma, dendrites, and axons of the tertiary structure) were evaluated separately to study the extension pattern of LBAS.

MATERIALS AND METHODS

Tissue Source

Tissue samples were collected at the Tokyo Metropolitan Geriatric Hospital, which, as previously reported (29), provides community-based medical service to the aged population. Between 2003 and 2006, 320 consecutive autopsy brains, spinal cords, and adrenal glands (29) from 180 men and 140 women were used for this study. Two hundred forty-seven of the 320 cases overlapped with our recent studies of LB pathology in the skin (35). The patients' age ranged from 52 to 104 years old, with a mean ± SD age of 81.5 ± 8.5 years. The postmortem interval ranged from 52 to 4,210 minutes, with a mean of 753 minutes.

Neuropathology

Brains and spinal cords were examined as reported previously (36). In brief, 1 hemisphere was preserved for biochemical and molecular studies, and the other portions were prepared for morphological studies. After fixation in formalin, the representative areas were embedded in paraffin. Serial 6-μm-thick sections were stained with hematoxylin and eosin (H&E) and Klüver-Barrera methods. Selected sections were further examined with modified methenamine (37) and Gallyas-Braak silver (38) staining for senile changes, Congo red for amyloid deposition, and elastica Masson trichrome stain for vascular changes.

Immunohistochemistry

Selected sections were immunostained using a Ventana 20NX autostainer (Ventana, Tucson, AZ), as previously

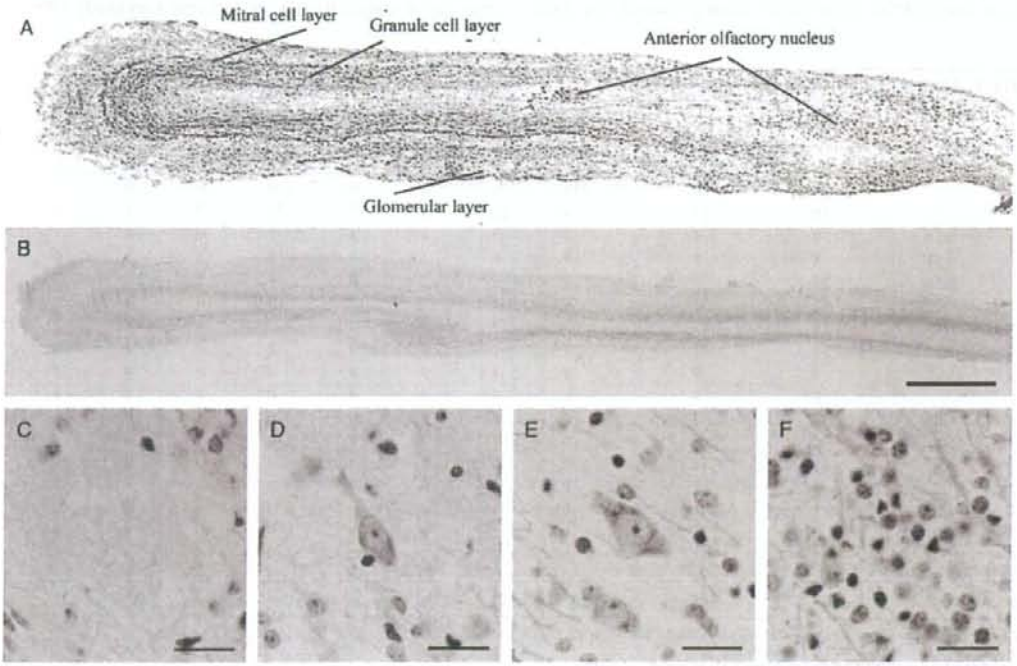

FIGURE 1. Schema and pathology of a sagittal section of the human olfactory bulb (OB). **(A)** Schema of the sagittal section of the human OB. Reproduced with permission from Elsevier © 2008 (34). **(B)** A representative sagittal section of the human OB. Scale bar = 1 mm. **(C)** Olfactory glomerulus. Scale bar = 25 μm. **(D)** Tufted cell. Scale bar = 25 μm. **(E)** Mitral cell. Scale bar = 25 μm. **(F)** Granule cell layer. Scale bar = 25 μm. **(B–F)** Klüver-Barrera method staining.

described (36). We immunostained representative sections as well as OBs from all patients with anti-phosphorylated α-synuclein (psyn; monoclonal, psyn no. 64 [39] and polyclonal PSer129 [40]), anti-phosphorylated tau (ptau; AT8, monoclonal; Innogenetics, Temse, Belgium), anti-β amyloid 11-28 (12B2, monoclonal; IBL, Maebashi, Japan), anti-ubiquitin (polyclonal, DAKO, Glostrup, Denmark), and anti-TH (monoclonal; Calbiochem-Novabiochem Corp, Darmstadt, Germany, and ImmunoStar, Hudson, WI) antibodies.

Evaluation of LBAS

To evaluate LBAS, we used immunohistochemistry with anti-psyn antibodies to screen OB sections, bilateral adrenal glands, medulla oblongata at the level of the dorsal motor nucleus of the vagus, upper pons at the level of the locus coeruleus, midbrain, amygdala, and posterior hippocampus. If anti-psyn immunoreactivity was observed in any of these regions, further studies with anti-psyn and ubiquitin antibodies were conducted on the anatomical structures as recommended by the original and revised DLB Consensus Guidelines (41, 42), PD staging by Braak et al (26), and our own previous work (39), which includes staining of CA2 of the hippocampus and intermediolateral column of the thoracic spinal cord (43), for staging of LBAS (42, 44). Our revised LB staging system (29) was applied to all patients as follows: Stage 0, no anti-psyn immunoreactive structure; Stage 0.5, Lewy dots or neurites only or fine granular cytoplasmic staining without any focal aggregates; Stage I, a few LBs confirmed by H&E staining, without neuronal loss (incidental LB disease); Stage II, abundant LBs with loss of pigmentation in the substantia nigra but without attributable parkinsonism or dementia (subclinical LB disease); Stage III, PD without dementia; Stage IV, DLB or PDD, transitional (limbic) form (DLBT or PDDT); and Stage V, DLB or PDD, neocortical (diffuse) form (DLBN or PDDN). Parkinson disease with dementia was differentiated from DLB by applying the "12-month" rule noted in the Consensus Guidelines (i.e. "dementia appears more than 1 year after the onset of parkinsonism") (41, 42). We subcategorized our Stage II patients into brainstem (B), transitional or limbic (T), and neocortical (N) forms based on Lewy score (41) and involvement of the intermediolateral column of the spinal cord (43) or the amygdala variant (A), as previously reported (27, 28). Stage 0.5 and Stage I patients were also subcategorized to the extent of LBAS localized in the brainstem (B), spreading to the limbic system (T) and neocortex (N) or preferentially present in amygdala (A), as previously reported.

Evaluation of Other Senile Changes and Neuropathologic Diagnosis

Neurofibrillary tangles (NFTs) were classified into Braak and Braak's (45) 7 stages (0–VI) and senile plaques (SPs) into 4 stages (0–C). Argyrophilic grains were classified into our 4 stages (0–III), as reported previously (46). The

TABLE 1. LBAS in the CNS and OB

BBAR LB Stage*	No.	LBAS in the OB	OB LBAS Grade: Periphery 0	Periphery 1	Periphery 2	Periphery 3	AON 0	AON 1	AON 2	AON 3	AON 4
0	218	0	218	0	0	0	218	0	0	0	0
0.5	30	17	15	10	3	2	21	7	1	1	0
0.5B	8	3	5	2	0	1	7	0	0	1	0
0.5T	8	5	3	3	1	1	5	2	1	0	0
0.5A	14	9	7	5	2	0	9	5	0	0	0
I	37	33	4	4	17	12	10	10	9	5	3
IB	16	13	***3***	***2***	***7***	***4***	***7***	***7***	***1***	***1***	***0***†
IT	14	13	***1***	***1***	***8***	***4***	***1***	***3***	***4***	***3***	***3***
IA	7	7	***0***	***1***	***2***	***4***	***2***	***0***	***4***	***1***	***0***
II	8	8	0	1	4	3	0	2	1	3	2
IIB	3	3	0	0	3	0	0	1	0	2	0
IIT	4	4	0	1	1	2	0	1	1	1	1
IIA	1	1	0	0	0	1	0	0	0	0	1
III	2	2	0	2	0	0	0	0	1	0	1
IIIT	1	1	0	1	0	0	0	0	0	0	1
IIIN	1	1	0	1	0	0	0	0	1	0	0
IV	11	11	0	2	7	2	**0**	**0**	**4**	**5**	**2**†
V	14	14	0	2	10	2	**0**	**0**	**1**	**2**	**11**
Total	320	85	237	21	41	21	249	19	17	16	19

Correlation between OB periphery and AON grade in BBAR LB Stages IB, IT, and IA (bold and italic group).
p values are 0.006, 0.754, and 0.125, respectively.
Correlation between BBAR LB Stages IV and V (bold group), $p = 0.005$.
*BBAR LB stage (29, 39, 44).
†, $p < 0.01$.
A, amygdala variant; AON, anterior olfactory nucleus; B, brainstem; BBAR, Brain Bank for Aging Research; LB, Lewy body; LBAS, LB-related α-synucleinopathy; N, neocortical; OB, olfactory bulb; T, transitional.

neuropathologic diagnosis of AD was based on our definition (47), which proposes a modification of the National Institute on Aging and Reagan Institute criteria (48). The diagnoses of dementia with grains and NFT-predominant forms of dementia were based on the definitions of Jellinger (49) and Jellinger and Bancher (50). The diagnosis of progressive supranuclear palsy was based on the National Institute of Neurological Disorders and Stroke criteria (51). The diagnosis of vascular dementia was based on the criteria of the National Institute of Neurological Disorders and Stroke-Association Internationale pour la Recherche et l'Enseignement en Neurosciences (52). With respect to combined pathologies, the diagnosis of AD plus DLB was based on Braak NFT Stage equal to or more than IV and SP Stage C (47), in combination with a Lewy score equal to or more than 4 with involvement of the CA2 of hippocampus and intermediolateral column of the spinal cord, as previously reported (29, 43).

Neuropathology of the OB

Both OBs were sampled at autopsy. One was snap frozen, and the other was fixed in 4% paraformaldehyde for 48 hours. A sagittal section was embedded in paraffin, and 6-μm-thick serial sections were stained with H&E, with Klüver-Barrera, or by immunohistochemistry with the same panel of antibodies previously described.

In addition, a double labeling immunofluorescence study was performed on selected sections of the OB. Deparaffinized sections were incubated simultaneously with polyclonal psyn (PSer129) and monoclonal anti-TH or polyclonal ptau (AP422, polyclonal, a gift from Dr Y. Ihara) (53) and monoclonal psyn no. 64. Primary antibodies were visualized with anti-rabbit Alexa 546 Fluor and anti-mouse immunoglobulin G Alexa 488 (Molecular Probes, Eugene, OR) with 4′,6-diamidino-2-phenylindole (DAPI) staining for the nucleus under a confocal laser microscope (LSM5, PASCAL, Carl Zeiss, Jena, Germany).

LB Grade of the OBs

The OB periphery and the AON (Fig. 1) were separately evaluated. The secondary olfactory structure included the soma and cell processes of mitral cells, tufted cells, granule cells, and periglomerular cells. Grading of α-synuclein pathology followed the revised DLB Consensus

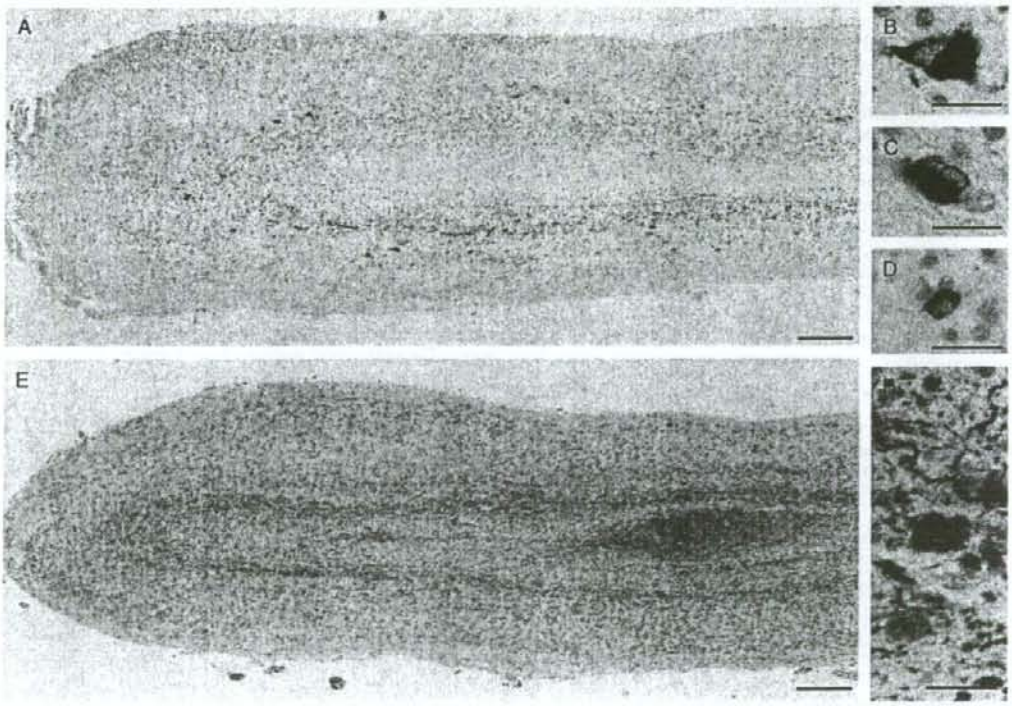

FIGURE 2. Lewy body (LB)–related α-synucleinopathy (LBAS) in different neuron populations in the olfactory bulb (OB). **(A)** Tissue from a patient with LBAS preferentially involving the periphery of the OB and surrounds the anterior olfactory nucleus (AON). Scale bar = 500 μm. **(B)** Mitral cell. Scale bar = 10 μm. **(C)** Tufted cell. Scale bar = 10 μm. **(D)** Granule cell. Scale bar = 10 μm. **(E)** Tissue from a patient with LBAS preferentially involving the AON. Scale bar = 500 μm. **(F)** AON neuron. Scale bar = 10 μm. **(A–F)** Immunohistochemistry with anti-phosphorylated α-synuclein antibody (psyn no. 64) counterstained with hematoxylin.

TABLE 2. Correlation Between LBAS Grades in the AON and in the Periphery of the OB

		LBAS Grade: AON		
		0	1	2≦
LBAS grade: Periphery	0	235	2*	0
	1	10	4	7
	2≦	4	13	45

$p = 0.004$.
*, complicated by coexistent Alzheimer disease pathology.
AON, anterior olfactory nucleus; LB, Lewy body; LBAS, LB-related α-synucleinopathy; OB, olfactory bulb.

TABLE 3. Correlations Between LBAS Grades in the AON and the OB Periphery With Clinical and Subclinical LB Disease

LBAS Grade	Periphery			
AON	0	1	2	3
0	0/0	0/10	0/2	0/2
1	0/2	0/4	0/10	0/3
2	0/0	1/2	3/7	1/8
3	0/0	2/2	5/11	0/3
4	0/0	3/3	9/11	2/5

The ratio represents the number of patients with clinical LB disease/the number of patients with either subclinical or clinical LB disease for each LBAS grade as described in the Materials and Methods section.
AON, anterior olfactory nucleus; LB, Lewy body; LBAS, LB-related α-synucleinopathy.

Guidelines (42). The classification of Tsuboi et al (54) for NFTs was applied. For SPs, we developed the following criteria: Grade 0, none; Grade 1, sparse dots; Grade 2, definite SPs, scattered; and Grade 3, abundant SPs.

Clinical Information

Clinical information, including the presence or absence of parkinsonism and cognitive state, was obtained from medical charts. The Mini-Mental State Examination (55) or the Hasegawa Dementia Scale (or its revised version [56]), and the Instrumental Activities of Daily Living (57) were used to evaluate cognitive function. The Clinical Dementia Rating (CDR) (58) was retrospectively determined by 2 independent board-certified neurologists. If the resulting ratings were in agreement, the score was accepted. If not, the neurologists reconciled their differences in the score after interviews with the patients' attending physicians and caregivers. Information about parkinsonism, bradykinesia, resting tremor, rigidity, and postural instability was obtained from neurological examinations. The presence of more than 2 of these clinical signs was interpreted as indicative of parkinsonism. The clinical diagnosis of AD was based on the criteria of the National Institute of Neurological and Communication Disorders and Stroke–Alzheimer Disease and Related Disorders Association (59).

Apolipoprotein E Genotype Analysis

We extracted genomic DNA from a freshly frozen kidney, measured the quantity of DNA with a spectrophotometer (Hitachi U2000, Tokyo, Japan), and adjusted it to 100 μg/mL. Tissues from all patients except for one (who had Creutzfeldt-Jakob disease) in the series were genetically examined in our laboratory. After polymerase chain reaction amplification, apolipoprotein E (APOE) genotyping was conducted with restriction enzyme *Hha*I, as described previously by Hixson and Vernier (60).

Statistical Analysis

Statistical comparison of LBAS grades in the AON and the OB periphery among patients at the Brain Bank for Aging Research (BBAR) (61) LB Stages IB, IT, IN, and IA (I, incidental LB disease; with extension of B, brainstem; T, transitional; N, neocortical; and A, amygdala as previously stated) was performed by the Friedman test. The Friedman test was used for comparison of categorical data. The Mann-Whitney U test was used for comparison of age at death. The relationships between LBAS grade in the OB and LBAS in the adrenal gland were assessed with the Mann-Whitney U test. Independent-sample *t*-tests were used for comparison of mean LBAS grade in the AON or the OB periphery and between Braak stages for SP and NFTs and the BBAR LB stage. The correlation between LBAS grade of the amygdala and of the AON or the OB periphery was assessed with Spearman rank correlation coefficient. Statistical comparison of LBAS grades, tau grades, and β-amyloid grades in AON and the periphery between APOE ε4 carriers and noncarriers using the Wilcoxon test. All statistical analyses were

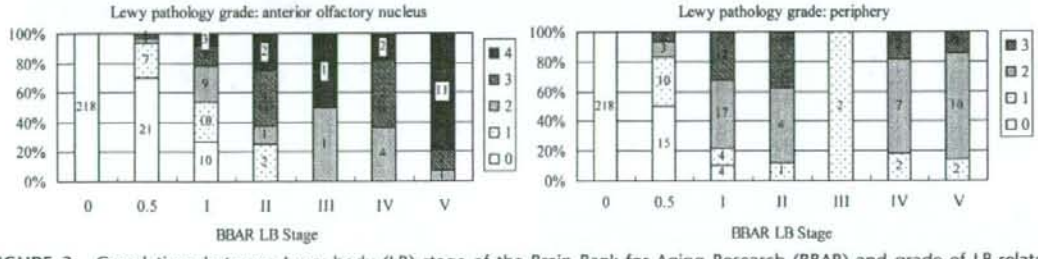

FIGURE 3. Correlations between Lewy body (LB) stage of the Brain Bank for Aging Research (BBAR) and grade of LB-related α-synucleinopathy (LBAS) in the anterior olfactory nucleus or the periphery of the olfactory bulb (OB). All patients with BBAR LB Stage ≥ II had LBAS in the OB.

TABLE 4. Correlations Between LBAS Grades in the OB and Degenerative Senile Changes in Other Areas of the CNS

	BBAR LB Stage			Braak SP Stage			Braak NFT Stage		
LBAS Grade	0.5–II	III–V	p	0–A	B–C	p	0–II	III–VI	p
AON	1.53	3.35	<0.001	1.76	2.33	0.051	2.05	2.12	0.814
Periphery	1.98	1.88	0.538	1.92	1.98	0.719	1.93	1.98	0.786

AON, anterior olfactory nucleus; BBAR, Brain Bank for Aging Research; LB, Lewy body (0.5–II, subclinical LB disease; III–V, Parkinson disease, Parkinson disease with dementia, and dementia with LBs); LBAS, LB-related α-synucleinopathy; NFT, neurofibrillary tangle; OB, olfactory bulb; SP, senile plaque.

performed using SPSS 15.0J for Windows (SPSS, Inc, Chicago, IL). The statistical significance level was set at $p < 0.05$.

RESULTS

Clinical Information

Among the 320 consecutive autopsy patients, 47 fit clinical criteria for parkinsonism (41). The CDR could retrospectively be assessed in 251 patients as follows: CDR 0, 95 patients; CDR 0.5, 41 patients; CDR 1, 31 patients; CDR 2, 15 patients; and CDR 3, 69 patients. The percentage of CDR equal to or greater than 0.5 was 62.2%.

Neuropathologic Diagnosis

The neuropathologic diagnoses consisted of AD (n = 25), vascular dementia (n = 20), DLB (n = 13), dementia with grains (n = 10), progressive supranuclear palsy (n = 6), PDD (n = 5), NFT-predominant form of dementia (n = 5), amyotrophic lateral sclerosis (n = 5), amyotrophic lateral sclerosis with dementia (n = 5), idiopathic hippocampal sclerosis (n = 3), PD (n = 2), and 1 case each of PD with Pick bodies, spinocerebellar ataxia 3/Machado-Joseph disease, multiple sclerosis, Kennedy-Alter Sung disease, Huntington disease, frontotemporal lobar degeneration with ubiquitinated inclusions, and Creutzfeldt-Jakob disease. Patients with combined pathologies included AD plus DLB (n = 6), AD plus vascular dementia (n = 2), dementia with grains plus NFT-predominant form of dementia (n = 2), and PDD plus progressive supranuclear palsy plus dementia with grains (n = 1). The remaining patients did not fulfill clinical and/or pathological criteria for neurodegenerative diseases.

The BBAR Staging for LBAS in the CNS, Including Spinal Cord

Lewy body–related α-synucleinopathy was found in 102 (31.9%) of the 320 patients (Table 1); the BBAR LB stages (29, 39, 44) were as follows: Stage 0, 218 patients; Stage 0.5, 30 patients; Stage I, 37 patients; Stage II, 8 patients; Stage III, 2 patients; Stage IV, 11 patients; and Stage V, 14 patients. The Stage IV patients included 4 of PDDT and 7 of DLBT, with 5 of the 7 DLBT patients having parkinsonism. The Stage V patients included 2 with PDDN and 12 with DLBN; 3 of the 12 DLBN patients had parkinsonism (42).

Incidence, Distribution, and Extent of LBAS in the OB

Lewy body–related α-synucleinopathy was detected in the OB of 85 (26.6%) of the 320 patients. The most frequent psyn-immunoreactive neuronal cells in the periphery were granule cells, followed by mitral cells, tufted cells, and periglomerular cells (Fig. 2). Lewy bodies in the OBs usually showed cortical-type morphological features, as reported previously (11); a few had halos.

Patients with LBAS in the OBs could be classified into 2 groups: one in which LBAS predominated in the AON (Fig. 2E) and the other in which LBAS predominated in the periphery of the OB (Fig. 2A). Very few psyn-positive neurites or dots were present in the olfactory nerve layer (where ramified axons of the bipolar receptor cells are present in the olfactory epithelium); therefore, LBAS in the periphery was found to reside mainly in the secondary olfactory structure. Lewy body–related α-synucleinopathy in

TABLE 5. Demography of 5 Patients With LB Identified Only in the OBs by H&E Stain

									LBAS							
								BBAR LB	OB Grade		Other Regions					
Patient	Age/Sex	Clinical Dx	CDR	BW, g	Np Dx	NFT	SP	Stage	AON	Periphery	dm	lc	sn	a	ca2	sc	adr
1	72/M	HCC	0.5	1351	unremarkable	I	A	0.5T	1	2	0	1	1	1	1	0	0
2	78/F	CRF dementia	2	1147	CVDE, VD	II	A	0.5B	3	3	1	1	1	1	0	0	0
3	89/M	Lung carcinoma post radiation therapy	1	1246	early AD	IV	C	0.5A	2	2	0	0	0	1	0	1	0
4	74/M	COPD	0.5	1413	AC	V	C	0.5T	2	3	1	1	1	1	1	0	0
5	82/F	AD	3	1123	AD	V	C	0.5A	1	2	0	0	0	1	0	0	0

a, amygdala; AC, Alzheimer disease changes; AD, Alzheimer disease; adr, adrenal gland; AON, anterior olfactory nucleus; BBAR, the Brain Bank for Aging Research; BW, brain weight; ca2, ca2 of the hippocampus; CDR, clinical dementia rating; COPD, chronic obstructive pulmonary disease; CRF, chronic renal failure; CVDE, clinically significant embolic cerebral vascular disease; dm, dorsal motor nucleus of vagus; Dx, diagnosis; F, female; H-E, hematoxylin and eosin; HCC, hepatic cell carcinoma; LB, Lewy body; LBAS, LB-related α-synucleinopathy; lc, locus caeruleus; M, male; NFT, Braak's stages for neurofibrillary tangles; Np, neuropathologic; OB, olfactory bulb; sc, spinal cord; sn, substantia nigra; SP, Braak's stages for senile plaques; VD, vascular dementia.

the AON was graded from 0 to 4 and LBAS in the OB periphery from 0 to 3. The AON Grades 3 and 4 patients were combined and analyzed with the Periphery Grade 3 patients.

Among the patients with LBAS in the OB, 14 were affected in the periphery alone and 2 in the AON alone. The latter 2 patients had AD and had very few psyn-immunoreactive granules in neuronal perikarya. In the earliest stage of LBAS in the OB, the periphery was more frequently involved than the AON (Table 2; $p = 0.004$).

Correlations Between LBAS in the OB and the CNS, Including Spinal Cord

Lewy body–related α-synucleinopathy in the OB was compared with LBAS in other locations of the CNS (Table 1; Fig. 3). The percentages of OB LBAS–positive patients at each BBAR LB stage were as follows: Stage 0, 0%; Stage 0.5, 56.7% (0.5B, 37.5%; 0.5T, 62.5%; 0.5A, 64.3%); Stage I, 89.2% (IB, 81.3%; IT, 92.9%; IA, 100%); and Stages II to V, 100% (Table 1; Fig. 3).

Among the 35 patients at BBAR LB Stage II or higher, 31 (88.6%) had LBAS in the adrenal glands. The 4 patients who lacked adrenal LBAS all had AD pathology. The average LBAS grade in the OB periphery of the 31 adrenal LBAS–positive patients was significantly greater ($p = 0.029$) than that of the 4 adrenal LBAS–negative patients. In contrast, the average LB grade in the AON of the 4 adrenal LBAS–negative patients was greater than that of the 31 adrenal LBAS–positive patients, although the difference was not significant ($p = 0.054$).

We further analyzed patients categorized as having BBAR LB Stage I. In the IB subgroup, the average LBAS grade of the periphery was significantly larger ($p < 0.01$) than that of the AON, but this difference was not significant in the IT and the IA subgroups ($p = 0.75$, $p = 0.13$; Table 1).

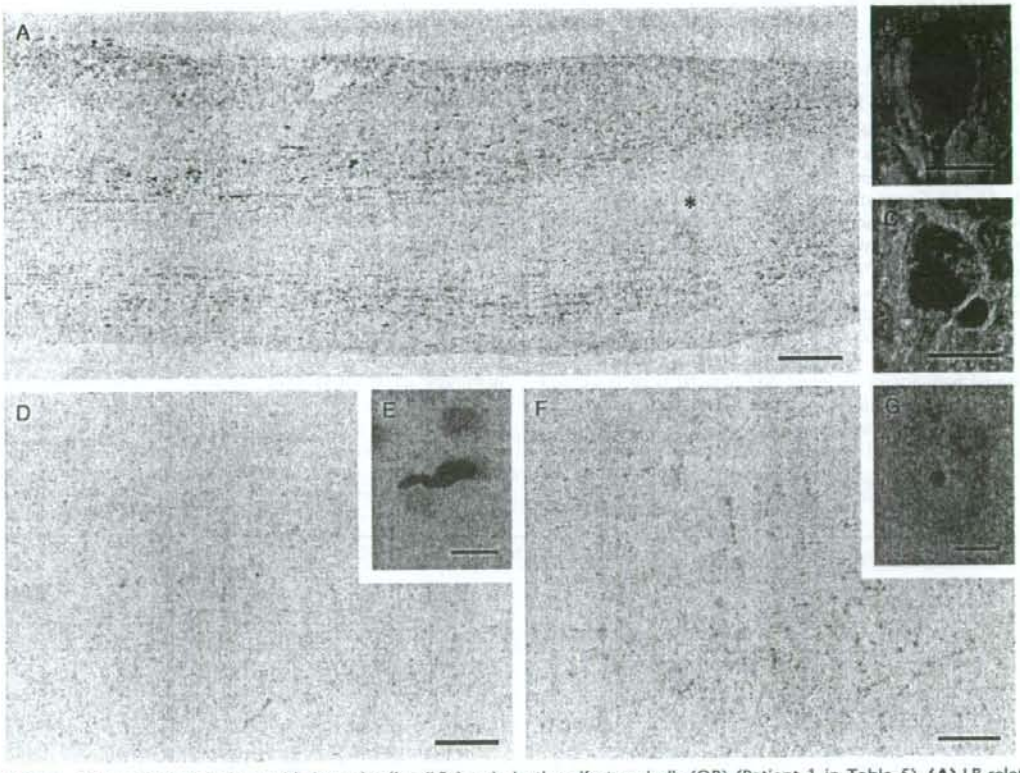

FIGURE 4. Tissue from a patient with Lewy bodies (LBs) only in the olfactory bulb (OB) (Patient 1 in Table 5). **(A)** LB-related α-synucleinopathy in the periphery of the OB (*anterior olfactory nucleus; immunohistochemistry (IH) with anti-phosphorylated α-synuclein antibody, visualized with diaminobenzidine. Scale bar = 200 μm. **(B)** LB in the periphery of the OB (H&E stain). Scale bar = 10 μm. **(C)** Intraneuronal perikaryal aggregates are stained by IH with anti-phosphorylated α-synuclein antibody (psyn no. 64). Scale bar = 10 μm. **(D)** IH with psyn no. 64 in the amygdala. Scale bar = 200 μm. **(E)** A single Lewy neurite is stained. Scale bar = 10 μm. **(F)** CA2 in the hippocampus shows almost no IH staining with psyn no. 64. Scale bar = 200 μm. **(G)** A fine granule is psyn no. 64 immunopositive in a neuron perikaryon. Scale bar = 10 μm.

All of the patients at BBAR LB Stage III or higher (PD/PDD/DLB) demonstrated high-grade LBAS in the AON. The mean grade of LBAS in the AON among patients at Stage V was significantly higher than that of Stage IV patients ($p = 0.005$; Table 1). One of 11 Stage IV patients and 5 of 14 Stage V patients fulfilled our pathological criteria of AD (47), and all of them (6/6, 100%) showed LBAS Grade 4 in the AON. In contrast, only 7 (36.8%) of 19 patients at Stages IV and V who did not fulfill our pathological criteria for AD showed LBAS Grade 4 in the AON.

We also compared patients with subclinical (≤Stage II) and clinical (≥Stage III) LB disease with regard to LBAS grade of the AON and the periphery of the OB (Table 3). The average LBAS grade in the AON, but not in the periphery, was significantly higher in clinical than in subclinical patients (Table 4).

LBAS in Amygdala and OB

Ninety-four (29.4%) of the 320 patients had LBAS in the amygdala. Among the 85 patients with positive LBAS in the OB, 83 had LBAS in the amygdala; the remaining 2 had Grade 1 LBAS in the periphery of the OB but not in the AON or amygdala. Five had Grade 1 LBAS in the amygdala but LBs in the OB (see later). All of the PD/PDD/DLB (BBAR LB Stages III, IV, and V) patients had Grade 4 LBAS in the amygdala, in accordance with the grading paradigm of the revised DLB Consensus Guidelines (42). The LBAS grade of the amygdala correlated more strongly with that of the AON than with that of the OB periphery (Spearman correlation coefficient, 0.853 and 0.521, respectively).

Correlations Between Braak's Stages for NFTs or SPs and LBAS in the OB

The mean LBAS grade of the AON was higher in Braak's SP Stages B and C than in Stages 0 and A ($p = 0.051$), although this difference was not statistically significant. Comparisons of other Braak stages did not reveal any statistical differences (Table 4).

Influence of APOE ε4 on Olfactory LBAS

The results of APOE genotyping of the 319 patients (excluding one with Creutzfeldt-Jakob disease) were as follows: 2 patients with the ε2/ε2 genotype; 12 with ε2/ε3; 1 with ε2/ε4; 247 with ε3/ε3; 51 with ε3/ε4; and 6 with ε4/ε4. The 57 APOE ε4 carriers had a significantly higher grade than the 262 noncarriers for tauopathy of the AON ($p = 0.011$) and anti-β amyloid amyloidosis of both the AON ($p < 0.001$) and the periphery ($p = 0.001$), but not for LBAS of the AON ($p = 0.80$) or the periphery ($p = 0.28$).

Correlation Between Incidence of LBAS of the OB and Age at Death

The mean age at death was 84.1 ± 8.1 years in OB-positive patients and 80.6 ± 8.6 years in OB-negative patients ($p = 0.014$). Although not statistically significant, the percentage of LBAS in the OB among those patients with LBAS involving the CNS also tended to increase with age: 73% (22/30) in the eighth decade, 87% (34/39) in the ninth decade, and 93% (25/27) in the 10th decade. No significant difference was noted between OB-positive and OB-negative patients with respect to sex.

Analysis of Data on the 5 Patients Who Had LBs Only in the OB by Routine H&E Stain

Among the 320 consecutive autopsy patients, 5 (1.6%) who were categorized as having BBAR LB Stage 0.5 had LBs recognized by H&E staining only in the OB (Table 5). No adrenal LBAS was found in these 5 patients. The group consisted of 3 men and 2 women, with a mean age at death of 79 years. One patient (Patient 1) had pure LBAS not markedly complicated by other senile changes or vascular

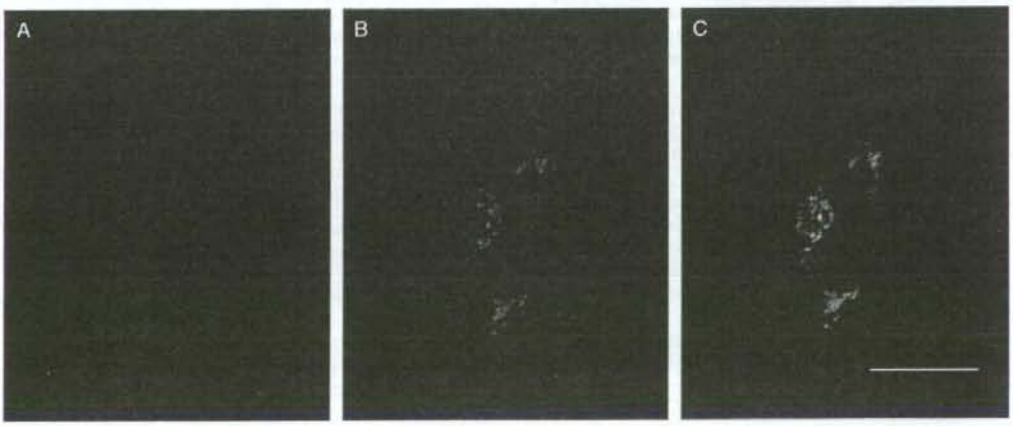

FIGURE 5. Colocalization of phosphorylated α-synuclein and tau in a neuron of the anterior olfactory nucleus visualized by confocal microscopy. There is little overlap in the staining. Patient 3 in Table 5. Scale bar = 10 μm. **(A)** Epitope of AP422 visualized with Alexa 546 Fluor (red). **(B)** Epitope of psyn no. 64, visualized with Alexa 488 Fluor (green). **(C)** Merged image. Nuclear stain with 4′,6-diamidino-2-phenylindole (DAPI) (blue).

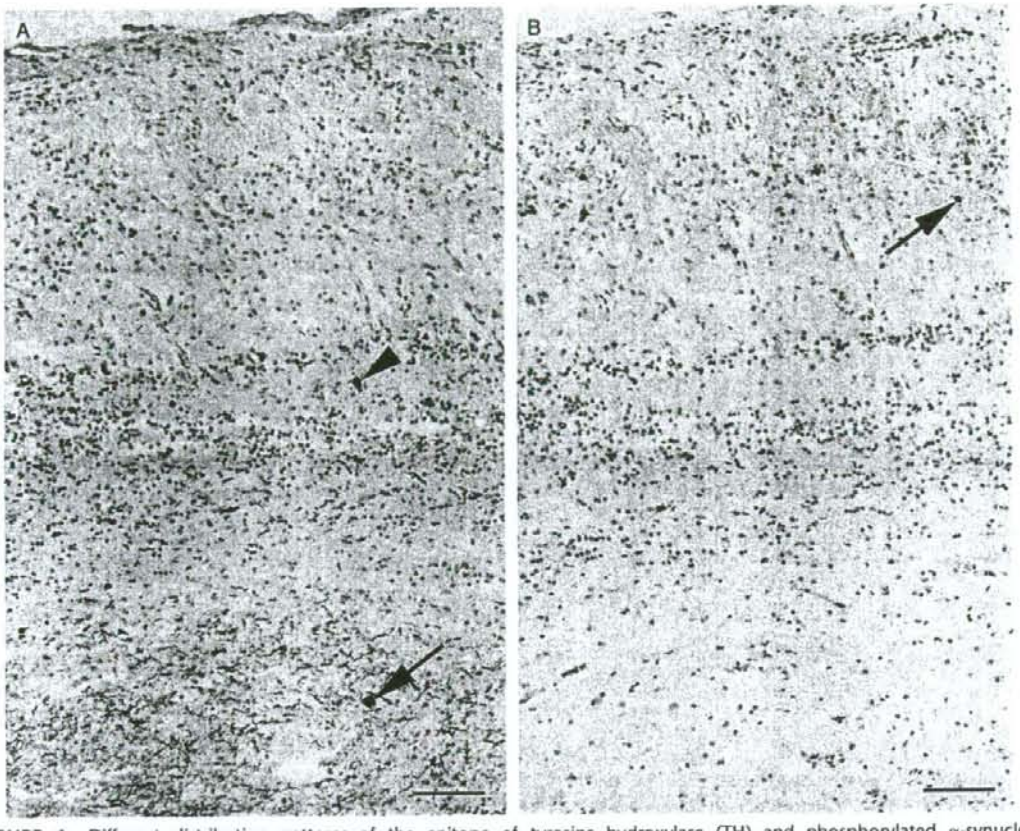

FIGURE 6. Different distribution patterns of the epitope of tyrosine hydroxylase (TH) and phosphorylated α-synuclein immunohistochemistry. **(A)** The epitope of anti-phosphorylated α-synuclein antibody was largely localized to mitral cells (arrowhead) and the granular cell layer and the anterior olfactory nucleus (arrow). Scale bar = 100 μm. **(B)** The epitopes of anti-TH antibodies were situated in periglomerular cells (arrow) and glomerulus.

lesions. Lewy body–related α-synucleinopathy preferentially involved the periphery of the OB (Fig. 4A), with a significant number of LBs (Figs. 4B, C). There were only a few anti-psyn–immunoreactive dots in the AON (Fig. 4A). Anti-psyn immunoreactivity was also present (but sparse) in the locus coeruleus, substantia nigra, amygdala (Figs. 4D, E), and CA2 of the hippocampus (Figs. 4F, G). Three of these patients had AD pathology, and all had colocalization of the epitopes of anti-psyn and ptau antibodies in neurons of the AON (Figs. 5A–C).

Correlation Between Anti-TH–Immunoreactive Neurons and LBAS

The epitopes of anti-TH antibodies were localized to periglomerular cells and very few granule cells in addition to the stratum album, as reported previously (62). The locations of the epitopes of anti-psyn antibodies were different from those of anti-TH antibodies and preferentially involved inner structures (Fig. 6). Very little colocalization of the epitopes of anti-psyn and TH antibodies could be detected (Figs. 7A–C).

DISCUSSION

There are 5 major findings in this study: 1) 26% of the consecutive autopsy patients from a general geriatric hospital had LBAS in the OB (peripheral OB, AON, or both); 2) LBAS always involved the OB in the advanced subclinical and clinical stages of LB disease; 3) in this aging population, LBs first appeared in the OB of 2% of patients; 4) LBAS in the OB appeared to extend from the periphery of the OB (secondary olfactory structure) to the AON (tertiary olfactory structure); and 5) LBAS in the amygdala was strongly correlated with LBAS in the OB; this correlation was more pronounced in the AON than in the periphery.

Subsequent to Kosaka et al (63), Braak et al (26) examined a cohort that consisted of incidental cases without

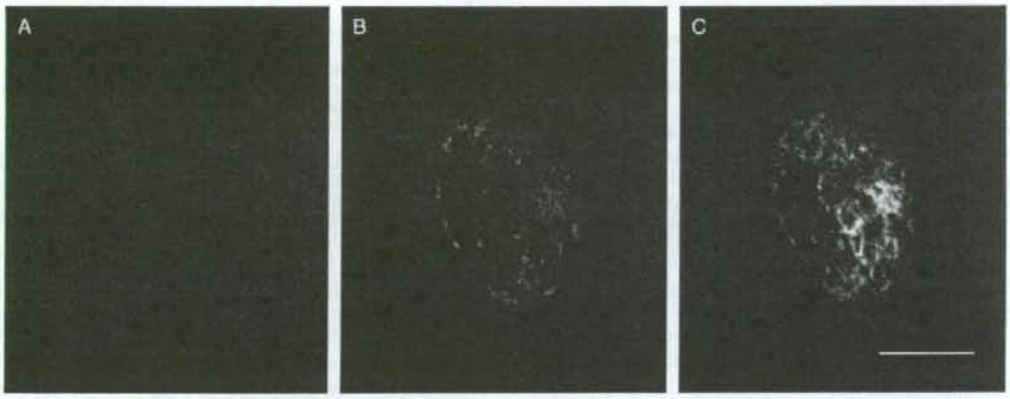

FIGURE 7. Epitopes of anti-phosphorylated α-synuclein antibody (PSer129) and anti–lltyrosine hydroxylase (TH) antibody were rarely colocalized. **(A)** Epitope of PSer129 visualized with Alexa 546 Fluor (red). Scale bar = 10 μm. **(B)** Epitope of TH visualized with Alexa 488 Fluor (green). **(C)** Merged image. Nuclear staining with 4′,6-diamidino-2-phenylindole (DAPI) (blue).

dementia and clinical PD patients with and without dementia, excluding AD and DLB by immunohistochemistry with anti–α-synuclein antibodies. They proposed a staging paradigm for LBAS, starting from the medulla oblongata, including the dorsal motor nucleus of the vagus, extending rostrally in the brainstem, spreading to the limbic system, and reaching the neocortex (26). Braak et al more recently reported findings in the OB and amygdala (30). The correlation between the Kosaka-Braak rostral extension pathway and the olfactory-amygdala pathway has yet to be determined. Three patients (Patients 1, 3, and 5 in Table 5) had LBAS in the OB but not in the dorsal motor nucleus of the vagus and did not follow the original staging of Braak et al (26). A difference between the study of Braak et al (30) and the present study is that although they evaluated both tertiary and secondary olfactory structures for the presence of LBAS, our examination of the various cell types and layers in the peripheral OB enabled us to conclude that the secondary olfactory structure is preferentially involved in early-stage LBAS.

Olfactory dysfunction is one of the initial manifestations in PD and occurs before motor dysfunction (64). An LB-type rapid eye movement sleep behavior disorder is also recognized to develop into PD, and a decrease in olfactory discrimination ability is also useful for the diagnosis of this disorder (65). We found that LBAS always involves the OB when LBAS includes degeneration of the substantia nigra, irrespective of the presence or absence of clinical parkinsonism or dementia; this suggests the morphological correlate of these clinical observations. Olfactory dysfunction is rarely recognized as a medical problem in the elderly in Japan, and we did not find descriptions of an impaired sense of smell in the retrospective investigation of medical charts.

Our findings that LBAS in the OB may start in the periphery and extend to the AON are in agreement with the results of Hubbard et al (66) who studied 79 OBs, 193 AON, and 201 amygdalae. Their specimens were independently registered in the Cambridge Brain Bank, and most of them had AD pathology. These studies may support the hypothesis of Hawkes et al (67) and Hawkes (68) that a neurotropic pathogen, probably viral, enters the brain through the olfactory pathway. Intranasal administration of the neurotoxin 1-methyl-4-phenyl-1,2,3,6-tetrahydropyridine to rats reduced the enzyme activity of TH in the OB and substantia nigra, resulting in a significant reduction in dopamine concentration in the OB and reproducing the clinical features of PD (69). In contrast, Huisman et al (24) reported that the total number of TH-immunoreactive neurons in the OB was twice as high in PD patients as in age- and sex-matched controls; they suggested that increased dopaminergic activity in the OB may lead to the suppression of olfactory information because of the inhibitory effect of dopamine on the transmission between olfactory receptor cells and mitral cells within the olfactory glomeruli (24). In the present study, the anatomical locations of LBAS and anti-TH–immunoreactive neurons rarely matched. The role of dopamine in olfactory dysfunction should, therefore, be further investigated to clarify these issues.

Our study also indicated a strong correlation between LBAS in the AON and LBAS in the amygdala. Three of 5 patients with LBs only in the OB also had AD pathology of NFT Stage IV or higher and we confirmed colocalization of the epitopes of anti-ptau and anti-psyn antibodies in the perikarya of AON neurons. Colocalization of these 2 epitopes has been reported in the amygdala, entorhinal cortex, and CA2 and 3 of hippocampus (70, 71), as well as in the OB (72). Fujishiro et al (72) first reported colocalization of α-synuclein and tau filaments in the OB with double enzyme immunocytochemistry and immunoelectron microscopy in the amygdala variant of LB disease complicated by AD. Because they screened AD patients with a considerable burden of LBAS in the amygdala and did not separately observe the changes in the periphery of the OB and AON, they could not determine in which direction(s) the LBAS spreads (Hiroki Fujishiro, the 49th Annual Meeting of the Japanese Society of Neuropathology, personal communication, Tokyo, May 2008). In contrast, Hubbard et al (66) proposed the

hypothesis that the spread of LBAS from the periphery of the OB to the AON and amygdala was independent. Taken together with these previous studies (66, 72), our present observations make it reasonable to conclude that in AD, LBAS first affects the periphery of the OB, spreads to the AON, and then reaches the amygdala. We also provide the first morphological evidence that the colocalization of tau and α-synuclein can first appear in the AON in AD with very little burden of α-synucleinopathy in the amygdala. Thus, we propose that the amygdala variant of LB disease should be renamed as the *olfactory-amygdala variant*.

The chief original observation of the present study is that we confirmed this pattern of spread in patients with pure Lewy pathology without AD. Moreover, our study clearly shows that the involvement of the periphery of the OB alone does not result in either Lewy body–associated parkinsonism or dementia. This suggests that the spread of LBAS in the AON and then into the amygdala may be required for the clinical manifestations of LB disease.

Our study also confirms the biologic significance of pale or LB seen in sections stained by H&E that corresponds to focal aggregates of immunoreactivity for phosphorylated α-synuclein. In the DLB revised Consensus Guidelines (42), which we followed, the presence of pale or LBs was determined to be equal to or more than Grade 2, whereas the presence of immunohistochemically visualized Lewy neurites or diffuse granular perikaryal neuronal staining alone, lacking pale or LBs, indicated Grade 1. Our results also indicate that the presence of LBs or pale bodies in AON (LBAS ≥ Grade 2) was correlated with a clinical presentation of LB disease (Table 3).

Thus, it is likely that the extension of LBAS from the OB periphery to the AON is essential for extension of LBAS from the OB to other areas of the CNS, including the amygdala. Recently, the presence of LBs in grafted fetal tissues in the striatum has been reported (73, 74), indicating the transmission of an LBAS pathogen through the neuronal network (67, 75, 76). Our present results are consistent with these new observations.

In conclusion, we show here that the OB is one of the initial anatomical sites affected by LBAS, and that its functional and morphological evaluation is useful for the neuropathologic diagnosis and clinical evaluation of LB disease.

ACKNOWLEDGMENTS

The authors thank Dr Takeshi Iwatsubo (Department of Neuropathology, University of Tokyo, Tokyo, Japan) and Dr Yasuo Ihara (Department of Neuropathology, Doshisha University, Kyoto, Japan) for the donation of antibody; Mr Naoo Aikyo, Mrs Mieko Harada, and Mrs Nobuko Naoi for the preparation of sections; and Dr Kinuko Suzuki for helpful discussions and comments. This study received the 2008 Moore Award at the annual meeting of the American Association for Neuropathologists, San Diego, CA, April 2008.

REFERENCES

1. Serizawa S, Ishii T, Nakatani H, et al. Mutually exclusive expression of odorant receptor transgenes. Nat Neurosci 2000;3:687–93
2. Buck L, Axel R. A novel multigene family may encode odorant receptors: A molecular basis for odor recognition. Cell 1991;65:175–87
3. Glusman G, Yanai I, Rubin I, et al. The complete human olfactory subgenome. Genome Res 2001;11:685–702
4. Bradley EA. Olfactory acuity to a pheromonal substance and psychotic illness. Biol Psychiatry 1984;19:899–905
5. Harrison PJ, Pearson RC. Olfaction and psychiatry. Br J Psychiatry 1989;155:822–28
6. Hurwitz T, Kopala L, Clark C, et al. Olfactory deficits in schizophrenia. Biol Psychiatry 1988;23:123–28
7. Moberg PJ, Agrin R, Gur RE, et al. Olfactory dysfunction in schizophrenia: A qualitative and quantitative review. Neuropsychopharmacology 1999;21:325–40
8. Turetsky BI, Moberg PJ, Yousem DM, et al. Reduced olfactory bulb volume in patients with schizophrenia. Am J Psychiatry 2000;157:828–30
9. Mesholam RI, Moberg PJ, Mahr RN, et al. Olfaction in neurodegenerative disease: A meta-analysis of olfactory functioning in Alzheimer's and Parkinson's diseases. Arch Neurol 1998;55:84–90
10. Daniel SE, Hawkes CH. Preliminary diagnosis of Parkinson's disease by olfactory bulb pathology. Lancet 1992;340:186
11. Hawkes CH, Shephard BC, Daniel SE. Olfactory dysfunction in Parkinson's disease. J Neurol Neurosurg Psychiatry 1997;62:436–46
12. Westervelt HJ, Stern RA, Tremont G. Odor identification deficits in diffuse Lewy body disease. Cogn Behav Neurol 2003;16:93–99
13. Sakuma K, Nakashima K, Takahashi K. Olfactory evoked potentials in Parkinson's disease, Alzheimer's disease and anosmic patients. Psychiatry Clin Neurosci 1996;50:35–40
14. ter Laak HJ, Renkawek K, van Workum FPA. The olfactory bulb in Alzheimer disease: A morphologic study of neuron loss, tangles, and senile plaques in relation to olfaction. In: *Alzheimer Disease and Associated Disorders*, vol. 8. New York, NY: Raven Press, 1994:38–48
15. Hawkes C. Olfaction in neurodegenerative disorder. Mov Disord 2003; 18:364–72
16. Ponsen MM, Stoffers D, Booij J, et al. Idiopathic hyposmia as a preclinical sign of Parkinson's disease. Ann Neurol 2004;56:173–81
17. Stiasny-Kolster K, Doerr Y, Moller JC, et al. Combination of "idiopathic" REM sleep behaviour disorder and olfactory dysfunction as possible indicator for alpha-synucleinopathy demonstrated by dopamine transporter FP-CIT-SPECT. Brain 2005;128:126–37
18. Ross GW, Abbott RD, Petrovitch H, et al. Association of olfactory dysfunction with incidental Lewy bodies. Mov Disord 2006;21:2062–67
19. Ross GW, Petrovitch H, Abbott RD, et al. Association of olfactory dysfunction with risk for future Parkinson's disease. Ann Neurol 2008; 63:167–73
20. Doty RL, Golbe LI, McKeown DA, et al. Olfactory testing differentiates between progressive supranuclear palsy and idiopathic Parkinson's disease. Neurology 1993;43:962–65
21. Thomann PA, Dos Santos V, Toro P, et al. Reduced olfactory bulb and tract volume in early Alzheimer's disease—a MRI study. Neurobiol Aging 2007 [Epub ahead of print]
22. Mueller A, Abolmaali ND, Hakimi AR, et al. Olfactory bulb volumes in patients with idiopathic Parkinson's disease a pilot study. J Neural Transm 2005;112:1363–70
23. Curtis MA, Kam M, Nannmark U, et al. Human neuroblasts migrate to the olfactory bulb via a lateral ventricular extension. Science 2007;315: 1243–49
24. Huisman E, Uylings HB, Hoogland PV. A 100% increase of dopaminergic cells in the olfactory bulb may explain hyposmia in Parkinson's disease. Mov Disord 2004;19:687–92
25. Kosaka K. Diffuse Lewy body disease in Japan. J Neurol 1990;237: 197–204
26. Braak H, Del Tredici K, Rub U, et al. Staging of brain pathology related to sporadic Parkinson's disease. Neurobiol Aging 2003;24:197–211
27. Hamilton RL. Lewy bodies in Alzheimer's disease: A neuropathological review of 145 cases using alpha-synuclein immunohistochemistry. Brain Pathol 2000;10:378–84
28. Uchikado H, Lin WL, DeLucia MW, et al. Alzheimer disease with amygdala Lewy bodies: A distinct form of alpha-synucleinopathy. J Neuropathol Exp Neurol 2006;65:685–97
29. Funimura Y, Ikemura M, Saito Y, et al. Analysis of the adrenal gland is useful for evaluating pathology of the peripheral autonomic nervous system in lewy body disease. J Neuropathol Exp Neurol 2007;66:354–62

30. Braak H, Muller CM, Rub U, et al. Pathology associated with sporadic Parkinson's disease—where does it end? J Neural Transm 2006:89–97
31. Carpenter M. Olfactory pathways, hippocampal formation, and the amygdala. *Core Text of Neuroanatomy*. Baltimore, MD: Williams & Wilkins, 1991:361–89
32. Cleland TA, Lister C. Central olfactory structures. In: Doty R, ed. *Handbook of Olfaction and Gustation*. New York, NY: Marcel Dekker, 2003:165–80
33. Kovacs T. Mechanisms of olfactory dysfunction in aging and neurodegenerative disorders. Ageing Res Rev 2004;3:215–32
34. Price JL. Olfaction. In: Paxinos G, Mai G, eds. *The Human Nervous System*. San Diego, CA: Elsevier Academic Press, 2004:1197–211
35. Ikemura M, Saito Y, Sengoku R, et al. Lewy body pathology involves cutaneous nerves. J Neuropath Exp Neurol 2008 In press.
36. Saito Y, Nakahara K, Yamanouchi H, et al. Severe involvement of ambient gyrus in dementia with grains. J Neuropathol Exp Neurol 2002; 61:789–96
37. Yamaguchi H, Haga C, Hirai S, et al. Distinctive, rapid, and easy labeling of diffuse plaques in the Alzheimer brains by a new methenamine silver stain. Acta Neuropathol (Berl) 1990;79:569–72
38. Gallyas F. Silver staining of Alzheimer's neurofibrillary changes by means of physical development. Acta Morphol Acad Sci Hung 1971; 19:1–8
39. Saito Y, Kawashima A, Ruberu NN, et al. Accumulation of phosphorylated alpha-synuclein in aging human brain. J Neuropathol Exp Neurol 2003;62:644–54
40. Fujiwara H, Hasegawa M, Dohmae N, et al. alpha-Synuclein is phosphorylated in synucleinopathy lesions. Nat Cell Biol 2002;4:160–64
41. McKeith IG, Galasko D, Kosaka K, et al. Consensus guidelines for the clinical and pathologic diagnosis of dementia with Lewy bodies (DLB): Report of the consortium on DLB international workshop. Neurology 1996;47:1113–24
42. McKeith IG, Dickson DW, Lowe J, et al. Diagnosis and management of dementia with Lewy bodies: Third report of the DLB Consortium. Neurology 2005;65:1863–72
43. Murayama S, Saito Y. Pathological diagnostic criteria of Lewy body dementia. In: *Symposium on Pathological Diagnosis of non-Alzheimer-type Dementia*. San Francisco, CA: XVIth International Congress of Neuropathology, 2006
44. Saito Y, Ruberu NN, Sawabe M, et al. Lewy body-related alpha-synucleinopathy in aging. J Neuropathol Exp Neurol 2004;63:742–49
45. Braak H, Braak E. Neuropathological stageing of Alzheimer-related changes. Acta Neuropathol (Berl) 1991;82:239–59
46. Saito Y, Ruberu NN, Sawabe M, et al. Staging of argyrophilic grains: An age-associated tauopathy. J Neuropathol Exp Neurol 2004;63:911–18
47. Murayama S, Saito Y. Neuropathological diagnostic criteria for Alzheimer's disease. Neuropathology 2004;24:254–60
48. The National Institute on Aging and Reagan Institute Working Group on Diagnostic Criteria for the Neuropathological Assessment of Alzheimer's Disease. Consensus recommendations for the postmortem diagnosis of Alzheimer's disease. Neurobiol Aging 1997;18:S1–2
49. Jellinger KA. Dementia with grains (argyrophilic grain disease). Brain Pathol 1998;8:377–86
50. Jellinger KA, Bancher C. Senile dementia with tangles (tangle predominant form of senile dementia). Brain Pathol 1998;8:367–76
51. Hauw JJ, Daniel SE, Dickson D, et al. Preliminary NINDS neuropathologic criteria for Steele-Richardson-Olszewski syndrome (progressive supranuclear palsy). Neurology 1994;44:2015–19
52. Roman GC, Tatemichi TK, Erkinjuntti T, et al. Vascular dementia: Diagnostic criteria for research studies. Report of the NINDS-AIREN International Workshop. Neurology 1993;43:250–60
53. Hasegawa M, Jakes R, Crowther RA, et al. Characterization of mAb AP422, a novel phosphorylation-dependent monoclonal antibody against tau protein. FEBS Lett 1996;384:25–30
54. Tsuboi Y, Wszolek ZK, Graff-Radford NR, et al. Tau pathology in the olfactory bulb correlates with Braak stage, Lewy body pathology and apolipoprotein epsilon4. Neuropathol Appl Neurobiol 2003;29:503–10
55. Folstein MF, Folstein SE, McHugh PR. "Mini-mental state." A practical method for grading the cognitive state of patients for the clinician. J Psychiatr Res 1975;12:189–98
56. Hasegawa KI, Inoue K, Moriya K. An investigation of dementia rating scale for the elderly. Seishin Igaku 1974;16:965–69
57. Lawton MP, Brody EM. Assessment of older people: Self-maintaining and instrumental activities of daily living. Gerontologist 1969;9:179–86
58. Hughes CP, Berg L, Danziger WL, et al. A new clinical scale for the staging of dementia. Br J Psychiatry 1982;140:566–72
59. McKhann G, Drachman D, Folstein M, et al. Clinical diagnosis of Alzheimer's disease: Report of the NINCDS-ADRDA Work Group under the auspices of Department of Health and Human Services Task Force on Alzheimer's Disease. Neurology 1984;34:939–44
60. Hixson JE, Vernier DT. Restriction isotyping of human apolipoprotein E by gene amplification and cleavage with HhaI. J Lipid Res 1990;31: 545–58
61. Murayama S, Saito Y, Kanemaru K, Tokumaru A, Ishii K, Sawabe M. Establishment of brain bank for aging research [In Japanese]. Nippon Ronen Igakkai zasshi 2005;42:483–89
62. Hoogland PV, Huisman E. Tyrosine hydroxylase immunoreactive structures in the aged human olfactory bulb and olfactory peduncle. J Chem Neuroanat 1999;17:153–61
63. Kosaka K, Yoshimura M, Ikeda K, et al. Diffuse type of Lewy body disease: Progressive dementia with abundant cortical Lewy bodies and senile changes of varying degree—a new disease? Clin Neuropathol 1984;3:185–92
64. Doty RL, Riklan M, Deems DA, et al. The olfactory and cognitive deficits of Parkinson's disease: Evidence for independence. Ann Neurol 1989;25:166–71
65. Postuma RB, Lang AE, Massicotte-Marquez J, et al. Potential early markers of Parkinson disease in idiopathic REM sleep behavior disorder. Neurology 2006;66:845–51
66. Hubbard PS, Esiri MM, Reading M, et al. Alpha-synuclein pathology in the olfactory pathways of dementia patients. J Anat 2007;211:117–24
67. Hawkes CH, Del Tredici K, Braak H. Parkinson's disease: A dual-hit hypothesis. Neuropathol Appl Neurobiol 2007;33:599–614
68. Hawkes CH. Parkinson's disease and aging: Same or different process? Mov Disord 2008;23:47–53
69. Prediger RD, Batista LC, Medeiros R, et al. The risk is in the air: Intranasal administration of MPTP to rats reproducing clinical features of Parkinson's disease. Exp Neurol 2006;202:391–403
70. Marui W, Iseki E, Kato M, et al. Pathological entity of dementia with Lewy bodies and its differentiation from Alzheimer's disease. Acta Neuropathologica 2004;108:121–28
71. Iseki E, Marui W, Kosaka K, et al. Frequent coexistence of Lewy bodies and neurofibrillary tangles in the same neurons of patients with diffuse Lewy body disease. Neurosci Lett 1999;265:9–12
72. Fujishiro H, Tsuboi Y, Lin WL, et al. Colocalization of tau and alpha-synuclein in the olfactory bulb in Alzheimer's disease with amygdala Lewy bodies. Acta Neuropathol (Berl) 2008;116:17–24
73. Kordower JH, Chu Y, Hauser RA, et al. Lewy body-like pathology in long-term embryonic nigral transplants in Parkinson's disease. Nat Med 2008;14:504–6
74. Li JY, Englund E, Holton JL, et al. Lewy bodies in grafted neurons in subjects with Parkinson's disease suggest host-to-graft disease propagation. Nat Med 2008;14:501–3
75. Braak H, Rub U, Gai WP, et al. Idiopathic Parkinson's disease: Possible routes by which vulnerable neuronal types may be subject to neuroinvasion by an unknown pathogen. J Neural Transm 2003;110:517–36
76. Braak H, Del Tredici K. Assessing fetal nerve cell grafts in Parkinson's disease. Nat Med 2008;14:483–85

ORIGINAL CONTRIBUTION

Development of a High-Throughput Microarray-Based Resequencing System for Neurological Disorders and Its Application to Molecular Genetics of Amyotrophic Lateral Sclerosis

Yuji Takahashi, MD, PhD; Naomi Seki, MD, PhD; Hiroyuki Ishiura, MD; Jun Mitsui, MD; Takashi Matsukawa, MD; Atsushi Kishino, MD; Osamu Onodera, MD, PhD; Masashi Aoki, MD, PhD; Nobuyuki Shimozawa, MD, PhD; Shigeo Murayama, MD, PhD; Yasuto Itoyama, MD, PhD; Yasuyuki Suzuki, MD, PhD; Gen Sobue, MD, PhD; Masatoyo Nishizawa, MD, PhD; Jun Goto, MD, PhD; Shoji Tsuji, MD, PhD

Background: Comprehensive resequencing of the causative and disease-related genes of neurodegenerative diseases is expected to enable (1) comprehensive mutational analysis of familial cases, (2) identification of sporadic cases with de novo or low-penetrant mutations, (3) identification of rare variants conferring disease susceptibility, and ultimately (4) better understanding of the molecular basis of these diseases.

Objective: To develop a microarray-based high-throughput resequencing system for the causative and disease-related genes of amyotrophic lateral sclerosis (ALS) and other neurodegenerative diseases.

Design: Validation of the system was conducted in terms of the signal-to-noise ratio, accuracy, and throughput. Comprehensive gene analysis was applied for patients with ALS.

Subjects: Ten patients with familial ALS, 35 patients with sporadic ALS, and 238 controls.

Results: The system detected point mutations with 100% accuracy and completed the resequencing of 270 kilobase pairs in 3 working days with greater than 99.9% accuracy of base calls, or the determination of base(s) at each position. Analysis of patients with familial ALS revealed 2 *SOD1* mutations. Analysis of the 35 patients with sporadic ALS revealed a previously known *SOD1* mutation, S134N, a novel putative pathogenic *DCTN1* mutation, R997W, and 9 novel variants including 4 nonsynonymous heterozygous variants consisting of 2 in *ALS2*, 1 in *ANG*, and 1 in *VEGF* that were not found in the controls.

Conclusion: The DNA microarray–based resequencing system is a powerful tool for high-throughput comprehensive analysis of causative and disease-related genes. It can be used to detect mutations in familial and sporadic cases and to identify numerous novel variants potentially associated with genetic risks.

Arch Neurol. 2008;65(10):1326-1332

With recent progress in human molecular genetics, many causative genes of inherited neurological diseases have been identified. In 2007, 667 neurological diseases were registered in the Online Mendelian Inheritance in Man database (http://www.ncbi.nlm.nih.gov/entrez/query.fcgi?db=OMIM) as diseases with identified causative genes. It should be noted that there are substantial nonallelic genetic heterogeneities in hereditary neurodegenerative diseases, including amyotrophic lateral sclerosis (ALS), Parkinson disease, Alzheimer disease, and hereditary spastic paraplegia. Thus, there is a strong demand for comprehensive mutational analysis of multiple causative genes in daily clinical practice.

Most neurodegenerative diseases are sporadic and their molecular etiologies remain unknown. Although genome-wide association studies (GWAS) using common variants of single nucleotide polymorphisms have been undertaken to identify the loci of disease-susceptibility genes, genetic risks associated with rare variants may not be captured by GWAS.[1] Identification of multiple rare variants, however, would need comprehensive resequencing of candidate genes. Furthermore, sporadic diseases may be caused by de novo mutations or low-penetrant mutations in the causative genes. Taken together, development of a comprehensive resequencing system of causative genes will be indispensable, not only to provide mutational analyses of multiple causative genes for familial diseases, but also to explore the molecular basis of sporadic diseases.

Author Affiliations are listed at the end of this article.

Table 1. Genes Tiled on Microarray TKYALS01

Gene	Product	Disease	Category	Sequence of Interest
SOD1	Superoxide dismutase 1	ALS	Causative	Exon
ALS2	Alsin	ALS	Causative	Exon
DCTN1	Dynactin	ALS	Causative	Exon
SLC1A2	Excitatory amino acid transporter 2	ALS	Related	Exon
SMN[a]	Survival motor neuron	ALS	Related	Mutation
LIF	Leukemia inhibitory factor	ALS	Related	Exon
VEGF[b]	Vascular endothelial growth factor	ALS	Related	Promoter (1586 bps), exon
RNF19	Dorfin	ALS	Related	Exon
CNTF[c]	Ciliary neurotrophic factor	ALS	Related	SNP
ADARB1	Adenosine deaminase, RNA-specific, 2	ALS	Related	Exon 6-exon 9
SPG7	Paraplegin	HSP	Causative	Exon
SNCG	Synuclein, γ	PD	Related	Promoter (700 bps), exon

Abbreviations: ALS, amyotrophic lateral sclerosis; bps, base pairs; HSP, hereditary spastic paraplegia; PD, Parkinson disease; SNP, single-nucleotide polymorphism.

[a] For *SMN*, the sequences at and around 6 bps inside exon 7, the only critical difference between *SMN1* and *SMN2*, were tiled to detect each deletion.

[b] The promoter sequences of *VEGF* were extensively included because previous studies indicated that the SNPs or promoter haplotypes are associated with ALS.

[c] For the SNP sequences, the variation sites and their 2 flanking base pairs were tiled.

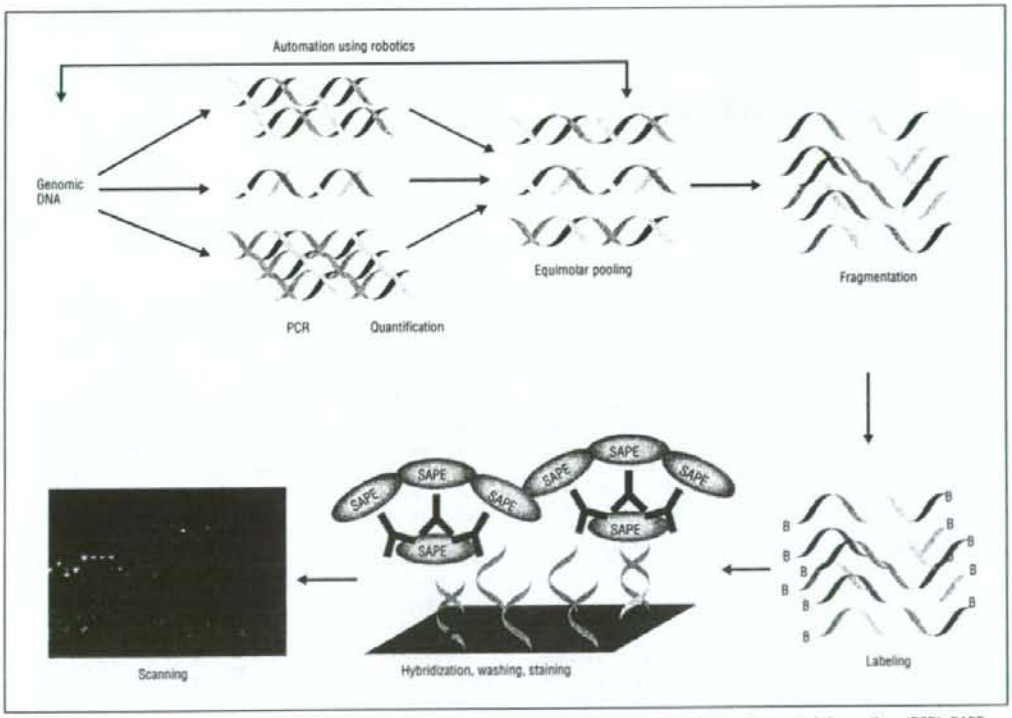

Figure 1. Procedures for microarray-based resequencing. A robotics system was introduced to manipulate numerous polymerase chain reactions (PCR). SAPE indicates streptoavidin-phycoerythrin; B, biotin.

A DNA microarray–based resequencing method has been invented to enable rapid and accurate nucleotide sequence analysis of multiple genes spanning 30 to 300 kilobase pairs.[2,3] We used this method to develop a comprehensive high-throughput resequencing system focusing on ALS as well as other neurodegenerative diseases. We herein describe the development of the microarray-based comprehensive resequencing system and its application to ALS genetics to validate the above-described concepts. We also discuss the implications of comprehensive resequencing for the molecular dissection of neurological diseases.

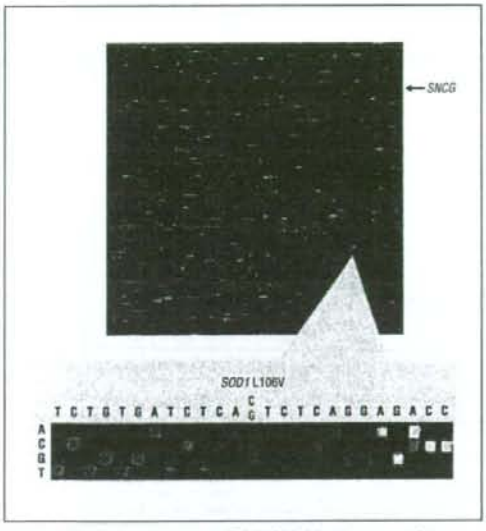

Figure 2. Whole view of microarray TKYALS01. A heterozygous point mutation of *SOD1*, L106V, was unambiguously identified.

METHODS

DESIGN OF MICROARRAYS

We have designed a microarray, TKYALS01, that primarily focuses on the causative genes of and genes related to ALS (**Table 1**). The sequences tiled on the microarray included the sequences of all of the exons and 12 flanking base pairs (bp) of the splice junctions. Promoter sequences were also included in the tiled sequences for genes whose expression levels were presumed to modify the disease processes.[4,5] In addition, another microarray, TKYPD01, was designed to focus on genes relevant to Parkinson disease, autosomal-dominant hereditary spastic paraplegias, and adrenoleukodystrophy (data not shown).

Because the principle of the resequencing microarray is based on sequencing by hybridization (SBH), it is crucially important to avoid cross-hybridization to increase the accuracy of resequencing. For this purpose, we conducted an "in silico" screening to compare the tiled sequences with a sliding 25-nucleotide window to detect the sequences with an identity exceeding 22 bases in the tiled sequences and optimized the design of the microarrays and polymerase chain reaction (PCR) primers.

PARTICIPANTS

Thirty-five patients with sporadic ALS and 10 patients with familial ALS, 7 with autosomal dominant mode of inheritance and 3 with affected siblings, were enrolled in this study. The diagnosis of ALS was based on El Escorial and the revised Airlie House diagnostic criteria. A total of 238 control genomic DNA samples were also used.

Thirty-six genomic DNA samples with previously determined mutations of *SOD1* (OMIM 147450), the causative gene of familial ALS,[6-9] or those of *ABCD1* (OMIM 300371), the causative gene of adrenoleukodystrophy,[10-13] were anonymized and subjected to analysis without prior information on the mutations.

All of the genomic DNA samples were obtained with written informed consent, and this research was approved by the institutional review board of the University of Tokyo.

PROCEDURES

Specific PCR primers were designed using the Primer3 Web site (http://frodo.wi.mit.edu/cgi-bin/primer3/primer3_www.cgi) (**eTable**, http://www.archneurol.com). Touch-down PCR protocols were used to enhance the specificity of PCR amplification (eTable). Each PCR product was quantified using PicoGreen (Molecular Probes, Eugene, Oregon), pooled equimolarly into 1 tube using a robotic system, BioMek FX (Beckman Coulter, Fullerton, California), and subjected to SBH according to the manufacturer's instructions (Affymetrix, Santa Clara, California) (**Figure 1**). The undetermined base calls were further analyzed by manual inspection of the signals. The resequencing of *ANG* (OMIM 105850) and the confirmation of all of the sequence variants determined by SBH were conducted by direct nucleotide sequence analysis using an automated DNA sequencer and BigDye Terminator version 3.1 (Applied Biosystems, Foster City, California). Analyses of frequency of variants in the controls were conducted by denatured high-performance liquid chromatography (Transgenomics, Omaha, Nebraska).

RESULTS

ESTABLISHMENT OF HIGH-THROUGHPUT COMPREHENSIVE RESEQUENCING SYSTEM

To evaluate the signal-to-noise ratio, all of the PCR amplicons for TKYALS01 except those for *SNCG* were subjected to hybridization to TKYALS01 and scanning. Simultaneous hybridization of the mixed PCR amplicons did not interfere with the signals and *SOD1* mutations were unambiguously identified (**Figure 2**). Furthermore, the areas where the probes for *SNCG* were tiled did not show any detectable signals, indicating that cross-hybridization was negligible.

As shown in **Figure 3**A, all of the point mutations were correctly identified, confirming the accuracy of SBH for detection of point mutations. The locations of the hemizygous *ABCD1* insertion/deletion mutations were also easily identified because the signals of the insertion/deletion sites and surrounding probes were undetectable (Figure 3B). Determination of the exact base changes required direct nucleotide sequence analysis. In contrast, none of the 4 heterozygous insertion/deletion mutations of *SOD1* were unambiguously detected without prior information on the mutations. Only the *SOD1* heterozygous deletion mutation del429TT was detectable by carefully evaluating the signal intensities (Figure 3C) because the signal intensities were moderately decreased at the deletion sites and the 12 flanking bases (Figure 3D).

By employing robotics to manipulate numerous PCR reactions, the resequencing of as many as 271 625 bp was easily accomplished in 3 working days with a total of 271 445 bp (99.93%) correctly called, confirming the high throughput of this system.

COMPREHENSIVE RESEQUENCING OF GENES RELEVANT TO ALS

The molecular diagnosis of 10 patients with familial ALS using this system revealed 2 *SOD1* mutations, including 1 novel mutation, K3E (**Figure 4**A), and 1 previously